ISTANBUL TECHNICAL UNIVERSITY ★ GRADUATE SCHOOL

# AN EXPONENTIAL WAVE INTEGRATOR SINE PSEUDO SPECTRAL METHOD FOR THE HIGHER ORDER BOUSSINESQ EQUATION

**M.Sc. THESIS**

**Melih Cem ÇANAK**

**Department of Mathematical Engineering**

**Mathematical Engineering Programme**

**JANUARY 2024**

**ISTANBUL TECHNICAL UNIVERSITY ★ GRADUATE SCHOOL**

# AN EXPONENTIAL WAVE INTEGRATOR SINE PSEUDO SPECTRAL METHOD FOR THE HIGHER ORDER BOUSSINESQ EQUATION

**M.Sc. THESIS**

**Melih Cem ÇANAK**
**(509201255)**

**Department of Mathematical Engineering**

**Mathematical Engineering Programme**

**Thesis Advisor: Prof. Dr. Gülçin Mihriye MUSLU**

**JANUARY 2024**

**İSTANBUL TEKNİK ÜNİVERSİTESİ ★ LİSANSÜSTÜ EĞİTİM ENSTİTÜSÜ**

# YÜKSEK MERTEBE BOUSSINESQ DENKLEMİNİN SAYISAL ÇÖZÜMLERİ İÇİN ÜSTEL SİNÜS SÖZDE SPEKTRAL YÖNTEMİ

**YÜKSEK LİSANS TEZİ**

**Melih Cem ÇANAK**
**(509201255)**

**Matematik Mühendisliği Anabilim Dalı**

**Matematik Mühendisliği Programı**

**Tez Danışmanı: Prof. Dr. Gülçin Mihriye MUSLU**

**OCAK 2024**

Melih Cem ÇANAK, a M.Sc. student of ITU Graduate School student ID 509201255 successfully defended the thesis entitled "AN EXPONENTIAL WAVE INTEGRATOR SINE PSEUDO SPECTRAL METHOD FOR THE HIGHER ORDER BOUSSINESQ EQUATION", which he prepared after fulfilling the requirements specified in the associated legislations, before the jury whose signatures are below.

| | | |
|---|---|---|
| **Thesis Advisor :** | **Prof. Dr. Gülçin Mihriye MUSLU**<br>Istanbul Technical University | ..... |
| **Jury Members :** | **Assoc. Prof. Dr. Ahmet KIRIŞ**<br>Istanbul Technical University | ..... |
| | **Assoc. Prof. Dr. Handan BORLUK**<br>Ozyegin University | ..... |

**Date of Submission :** **29 December 2023**
**Date of Defense :** **15 January 2024**

***To my family,***

## FOREWORD

I would like to express my sincere gratitude to my advisor Prof. Dr. Gülçin Mihriye Muslu who not only meticulously guided me at every stage of my thesis work but also spared her valuable time to help me become a better academician. I want also to show my gratefulness to my family for always supporting me. This study has been supported by the Scientific and Technological Research Council of Turkey (TUBITAK) under grant 2210-A.

January 2024

Melih Cem ÇANAK
(Research Assistant)

**TABLE OF CONTENTS**

**ABBREVIATIONS**

| | |
|---|---|
| **PDE** | **:** Partial Differential Equation |
| **HBq** | **:** Higher-Order Boussinesq |
| **IBq** | **:** Improved Boussinesq |
| **EWI-SP** | **:** Exponential Wave Integrator Sine Pseudo-Spectral |

## LIST OF FIGURES

**Page**

## AN EXPONENTIAL WAVE INTEGRATOR SINE PSEUDO SPECTRAL METHOD FOR THE HIGHER ORDER BOUSSINESQ EQUATION


### SUMMARY

In this thesis, it is aimed to derive a new scheme for the numerical solutions of the higher-order Boussinesq equation on a bounded domain $\Omega = (a,b)$ with initial and homogeneous boundary conditions given by

$$\begin{cases} u_{tt} = u_{xx} + \eta_1 u_{xxtt} - \eta_2 u_{xxxxtt} + (f(u))_{xx}, \quad x \in \Omega, \quad t > 0, \\ u(x,0) = u_0(x), \quad u_t(x,0) = u_1(x), \\ u(a,t) = u(b,t) = 0, \quad t \geq 0, \end{cases}$$

where $u(x,t)$ is the unknown function, $\eta_1$ and $\eta_2$ are real positive constants and $f \in C^{\infty}(\mathbb{R},\mathbb{R})$.

The higher-order Boussinesq equation reduces to the improved Boussinesq equation when $\eta_1 = 1$ and $\eta_2 = 0$. Although there are many analytical and numerical studies for the improved Boussinesq equation in the literature, there are few studies because the higher-order Boussinesq equation includes the sixth-order derivative term $u_{xxxxtt}$.

The thesis includes the following sections:

In Section 1, the purposes of the thesis, the literature review and the hypothesis of the thesis are presented.

In Section 2, some definitions related to sine pseudo-spectral discretization and Sobolev Spaces are provided. In addition, inequalities used in the proof of the main theorem, such as the discrete Gronwall's lemma and Young's inequality, are introduced.

In Section 3, a new exponential wave integrator sine pseudo-spectral method for the higher-order Boussinesq equation is derived. The sine pseudo-spectral discretization

$$u_M(x,t_n+s) = \sum_{l=1}^{M-1} \widehat{u}_l(t_n+s)\sin(\mu_l(x-a)), \qquad x \in \Omega, s \in \mathbb{R}$$

is used to find the numerical solutions of the higher-order Boussinesq equation. Here, $\widehat{u}_l(t_n+s)$ is the continuous sine coefficient and $\mu_l = \frac{\pi l}{b-a}$. The higher-order Boussinesq equation is reduced to the second-order non-homogeneous ordinary differential equation by using this discretization. $\widehat{u}_l(t_n+s)$ is obtained by solving the second-order differential equation. Then, the approximate solution $u_M(x,t)$ is found.

In Section 4, we rigorously carry out error analysis and establish error bounds in the Sobolev spaces. The main theorem shows that the method has fourth-order accuracy in time and spectral accuracy in space.

In Section 5, the scheme is tested by the exact solution of the higher-order Boussinesq equation. The performance of the scheme is illustrated by examining the propagation of the single solitary wave, single wave splitting and head-on collision of two solitary waves.

In Section 6, the outcome of the thesis is summarized.

# YÜKSEK MERTEBE BOUSSINESQ DENKLEMİNİN SAYISAL ÇÖZÜMLERİ İÇİN ÜSTEL SİNÜS SÖZDE SPEKTRAL YÖNTEMİ

## ÖZET


Bu tezde yüksek mertebe Boussinesq denklemi için tanımlanmış başlangıç ve sınır değer probleminin

$$\begin{cases} u_{tt} = u_{xx} + \eta_1 u_{xxtt} - \eta_2 u_{xxxxtt} + (f(u))_{xx}, \quad x \in \Omega, \quad t > 0, \\ u(x,0) = u_0(x), \quad u_t(x,0) = u_1(x), \\ u(a,t) = u(b,t) = 0, \quad t \geq 0, \end{cases}$$

çözümlerinin sayısal olarak bulunması için yeni bir yöntem bulunması ve bu yöntemin yakınsaklık analizinin yapılması hedeflenmiştir. Burada $u(x,t)$ bilinmeyen fonksiyon, $\eta_1$ ve $\eta_2$ pozitif sabitler ve $f \in C^\infty(\mathbb{R},\mathbb{R})$, $\Omega = (a,b)$ olarak göz önüne alınacaktır.

$\eta_1 = 1$ and $\eta_2 = 0$ olduğunda yüksek mertebeden Boussinesq denklemi düzgünleştirilmiş Boussinesq denklemine indirgenir. Literatürde düzgünleştirilmiş Boussinesq denklemi ile ilgili birçok analitik ve sayısal çalışma olmasına rağmen, yüksek mertebe Boussinesq denkleminin altıncı mertebeden türev terimi $u_{xxxxtt}$ içermesi sebebiyle az çalışma bulunmaktadır.

Tez aşağıdaki bölümleri içermektedir:

Bölüm 1'de tezin amacı, literatür araştırması ve tezin hipotezleri sunulmuştur.

Bölüm 2'de sinüs sözde-spektral ayrıklaştırması ve Sobolev uzayları ile ilgili bazı tanımlar verilmiştir. Buna ek olarak, ana teoremin ispatı için gerekli ayrık Gronwall eşitsizliği ve Young eşitsizliği gibi bazı eşitsizlikler de bu bölümde sunulmuştur.

Bölüm 3'te yüksek mertebe Boussinesq denkleminin sayısal çözümlerini elde etmek için yeni bir sinüs sözde-spektral yöntemi türetilmiştir. Sinüs sözde-spektral ayrıklaştırması kullanılarak yaklaşık çözüm

$$u_M(x,t_n+s) = \sum_{l=1}^{M-1} \widehat{u_l}(t_n+s)\sin(\mu_l(x-a)), \qquad x \in \Omega, s \in \mathbb{R}$$

olarak yazılabilir. Burada $\widehat{u_l}(t_n+s)$ sürekli sinüs Fourier katsayıları ve $\mu_l = \frac{\pi l}{b-a}$ olarak verilmiştir. Sinüs sözde-spektral ayrıklaştırılması yüksek mertebe Boussinesq denklemine uygulandığında

$$\frac{d^2}{ds^2}\widehat{u_l}(t_n+s) + \theta_l^2 \widehat{u_l}(t_n+s) + \theta_l^2 \widehat{(f_M^n)}_l(s) = 0, \qquad s \in \mathbb{R}$$

denklemi elde edilir. Bu sayede iki değişkenli kısmı diferansiyel denklem problemi her zaman adımı için ikinci-mertebe homojen olmayan adi diferansiyel

denklemler problemine indirgenir. Burada $f_M^n(x,s) = P_M f(u_M(x,t_n+s))$ ve $\theta_l = \mu_l/\sqrt{1+\eta_1\mu_l^2+\eta_2\mu_l^4}$ olarak tanımlanmıştır. İkinci-mertebe homojen olmayan adi diferansiyel denklemler parametrelerin değişimi yöntemiyle çözülebilir. Elde edilen çözümler ve çözümlerin türevi doğrusal olmayan terimle ilişkili bir integral içermektedir. Zamanda dördüncü mertebeden doğruluk elde edilebilmesi için integraller Simpson yöntemi yardımıyla çözülmüştür. Sürekli sinüs Fourier katsayıları, ayrık sinüs Fourier katsayıları ile yer değiştirilerek

$$\begin{aligned}
\widetilde{u_l^{n+1}} &= \cos(2\theta_l\tau)\widetilde{u_l^{n-1}} + \frac{\sin(2\theta_l\tau)}{\theta_l}\widetilde{\dot{u}_l^{n-1}} \\
&\quad -\frac{\theta_l\tau}{3}\Big[\sin(2\theta_l\tau)\widetilde{f_l^{n-1}} + 4\sin(\theta_l\tau)\widetilde{f}_l^{n}\Big], \\
\widetilde{\dot{u}_l^{n+1}} &= -\theta_l\sin(2\theta_l\tau)\widetilde{u_l^{n-1}} + \cos(2\theta_l\tau)\widetilde{\dot{u}_l^{n-1}} \\
&\quad -\frac{\theta_l^2\tau}{3}\Big[\cos(2\theta_l\tau)\widetilde{f_l^{n-1}} + 4\cos(\theta_l\tau)\widetilde{f}_l^{n} + \widetilde{f_l^{n+1}}\Big]
\end{aligned}$$

şeması türetilmiştir. Buna göre $n+1$ zaman adımındaki sayısal çözüm ve türevi $n$ ve $n-1$ zaman adımlarındaki çözümler ve türevleri kullanılarak hesaplanabilir. Yöntem $n=1$ için kullanılamadığından, Taylor açılımı yardımıyla $n=1$ zaman adımında çözüm ve türevinin

$$\begin{aligned}
\widetilde{u}_l^1 &= \widetilde{u}_l^0 + \tau\widetilde{\dot{u}}_l^0 - \frac{\theta_l^2\tau^2}{2}\Big[\widetilde{u}_l^0 + \widetilde{f}_l^0\Big] - \frac{\theta_l^2\tau^3}{6}\Big[\widetilde{\dot{u}}_l^0 + \widetilde{\dot{f}}_l^0\Big] \\
\widetilde{\dot{u}}_l^1 &= \Big(\frac{1}{2\tau} + \frac{\theta_l^2\tau}{12}\Big)\Big(\widetilde{u}_l^2 - \widetilde{u}_l^0\Big) + \frac{\theta_l^2\tau}{12}\Big(\widetilde{f}_l^2 - \widetilde{f}_l^0\Big)
\end{aligned}$$

şeklinde hesaplanabileceği gösterilmiştir. $n=0$ ve $n=1$ zaman adımındaki çözümler kullanılarak iterasyona başlanabilir. Sinüs Fourier katsayılarının her zaman adımında elde edilmesi ile $u_M(x,t_n)$ yaklaşık çözümü inşaa edilmiştir.

Bölüm 4'te türetilen sayısal yöntemin kullanılmasıyla elde edilen yaklaşık çözümler için Sobolev uzaylarında hata için bir üst sınır Teorem 1'de verilmiştir. Bununla birlikte, elde edilen yöntemin en genel doğrusal olmayan terime sahip yüksek mertebe Boussinesq denklemi için zamanda dördüncü mertebeden, uzayda eksponansiyel mertebeden doğruluğa sahip olduğu gösterilmiştir.

Bölüm 5'te bazı sayısal örnekler sunulmuştur. Yüksek mertebe Boussinesq denkleminde bulunan doğrusal olmayan terim $f(u) = u^p$ şeklinde kuvvet tipinde olduğunda yalnız dalga çözümleri analitik olarak bilinmektedir. Bölüm 5.1'de türetilen sayısal yöntem kullanılarak $p=2$ ve $p=3$ için yalnız dalga çözümleri elde edilmiş ve bulunan sayısal çözümler analitik çözümlerle kıyaslanarak yöntem test edilmiştir. Elde edilen hataların Teorem 1'de verilen teorik sonuçları desteklediği görülmüştür. Buna ek olarak türetilen yöntem yüksek mertebe Boussinesq denkleminin çözümlerinin uzun zaman davranışı incelenerek hataların zaman içerisindeki değişimi ve korunan kütle büyüklüğünün değişimi sunulmuştur. Bölüm 5.2 ve 5.3'te tek dalganın ayrılması ve iki yalnız dalganın çarpışması problemleri kuvvet tipinde doğrusal olmayan terime

sahip yüksek mertebe Boussinesq denklemi için sayısal olarak elde edilmiştir. Bu problemler için analitik çözümler bilinmediğinden hatalar hesaplanamamış, korunan kütle büyüklüğünün değişimi sunulmuştur.

Bölüm 6'da tezden elde edilen sonuçlar sunulmuştur. Tezde türetilen yöntemin zamanda dördüncü mertebeden doğruluğa sahip olması daha az hesaplama kapasitesiyle daha doğru sonuçlar bulunmasını sağlamaktadır. Ayrıca türetilen yöntemin açık olması hesaplama maliyetinin düşük olmasını sağlamaktadır. Bununla birlikte türetilen yöntemin sadece yüksek mertebe Boussinesq denklemi için değil sinüs sözde-spektral şema yardımıyla ikinci-mertebe homojen olmayan adi diferansiyel denklemlere indirgenebilen diğer denklemler için de kullanılabileceği öngörülmektedir.

# 1. INTRODUCTION

## 1.1 Purpose of Thesis

In this thesis, we study the higher-order Boussinesq (HBq) equation

$$u_{tt} = u_{xx} + \eta_1 u_{xxtt} - \eta_2 u_{xxxxtt} + (f(u))_{xx} \tag{1.1}$$

with initial and homogeneous boundary conditions. Here, $u(x,t)$ is the unknown function, $\eta_1$ and $\eta_2$ are real positive constants. We consider a single power-type nonlinearity as $f(u) = u^p$. The purpose of the thesis is to derive a new numerical method for finding numerical solutions to equation (1.1) and to establish error bounds in the Sobolev spaces.

## 1.2 Literature Review

Rosenau first derived the HBq equation for modelling the continuum limit of a dense chain of particles with elastic couplings in [1]. The propagation of longitudinal waves in an infinite elastic medium with nonlinear and non-local properties is also described by the HBq equation in [2]. Choosing the parameter $\eta_2 = 0$, the equation (1.1) reduces the improved Boussinesq equation

$$u_{tt} = u_{xx} + \eta_1 u_{xxtt} + (f(u))_{xx}, \tag{1.2}$$

which models the water wave problem with zero surface tension [3]. The most well-known classical Boussinesq equation [4] is given by

$$u_{tt} = u_{xx} + \alpha u_{xxxx} + (u^2)_{xx}. \tag{1.3}$$

When $\alpha = -1$, (1.3) is referred as the "good" Boussinesq equation, and when $\alpha = 1$, it is referred as the "bad" Boussinesq equation. Bogolubsky revealed that contrary to the "good" Boussinesq equation, the "bad" Boussinesq equation is unstable under short-wave perturbation and has no local well-posedness result in [5]. The improved

Boussinesq equation has been shown as an approach for the "bad" Boussinesq equation by replacing the term $u_{xxxx}$ with $u_{xxtt}$, which is physically stable [5,6].

Regarding the existence of local/global solutions of the Cauchy problem concerning (1.1), the authors in [2] used the fixed-point technique for the initial data in $H^s$ with $s > 1/2$. The local and global existence of solutions to the initial and boundary value problems corresponding to the initial data in *(i)* the Sobolev space $W^{3,\infty}(0,1)$ for the nonlinear function $f(s) \in C^1(\mathbb{R})$ with $f(0) = 0$ and *(ii)* the Sobolev space $H^{m+3}(0,1)$, $m \geq 1$ for the nonlinear function $f(s) \in C^m(\mathbb{R})$ with $f(0) = 0$ are established in [7]. Considering a general nonlinearity, the group classification and exact solutions of the HBq equation are obtained in [8].

From the numerical point of view, a variety of numerical schemes for approximating the time evolution of the solutions of the "good" Boussinesq equation have been proposed including the finite difference methods [9,10], pseudo-spectral methods [11,12], splitting methods [13] and the exponential wave integrators [14]. There are also a large number of studies in the literature on the IBq equation involving finite difference methods [9,15], finite element methods [16,17], spectral methods [18], meshless methods [19], Runge-Kutta type exponential integrators [20], energy preserving methods [21,22] and exponential wave integrators [23]. To the best of our knowledge, there is only one numerical study [24] in the literature considering the HBq equation. The convergence of the semi-discrete scheme is only proved in [24] and the authors focus on the quadratic nonlinearity.

The exponential wave integrator pseudo-spectral method has recently become very popular for solving time-dependent PDEs due to its superior properties. The method can be implemented efficiently by applying the fast discrete Fourier or Sine transform for the spatial discretization combined with an exponential wave integrator based on some efficient quadrature rules. Bao and Dong proposed a method based on the Fourier pseudo-spectral approach to spatial discretization followed by a Gautschi-type exponential integrator for the Klein-Gordon equation in the non-relativistic limit regime [25]. Zhao studied an exponential wave integrator sine pseudo-spectral method for solving the Klein-Gordon-Zakharov system

in [26] and an exponential wave integrator Fourier pseudo-spectral method for solving symmetric regularized-long-wave equation in [27]. The numerical method is based on a Deuflhard-type and Gautschi-type exponential wave integrator for temporal integrations, respectively. Exponential wave integrator methods are also applied successfully for the nonlinear Schrödinger equation [28], the extended Fisher-Kolmogorov equation [29]. As far as we know, the methods given in above mentioned studies have second-order accuracy in time and spectral accuracy in space. A fourth-order exponential wave integrator Fourier pseudo-spectral method for the nonlinear Dirac equation and the nonlinear Schrödinger equation are proposed in [30] and [31], respectively. For approximating the integral terms, the authors in [30,31] use the Simpson quadrature formula. However, the proposed schemes are implicit schemes that require solving a nonlinear system for each step. Ji and Zhang presented a fourth-order exponential wave integrator Fourier pseudo-spectral method for solving the Klein-Gordon equation in [32]. The scheme is explicit and the corrected trapezoidal formula is used for approximating the integral term. They proved the fourth-order convergence in time under the restriction $\tau \leq \frac{\pi h}{3\sqrt{2\pi^2+h^2}}$, where $\tau$ is the time step and $h$ is the spatial step size. Wang and Zhao introduce a group of symmetric Gautschi-type exponential wave integrators for the Klein-Gordon equation [33] in nonrelativistic limit regime. The scheme has fourth-order convergence in time. However, this scheme involves a rather complicated procedure due to the approximation of the second-order time derivative of the nonlinear function.

### 1.3 Hypothesis

To the best of our knowledge, the exponential wave integrator methods applied to the "good" Boussinesq equation [14] and the improved Bousinesq equation [23] are both second-order accurate in time. In order to demonstrate higher-order calculations for the Boussinesq-type equations, we derive a new fourth-order accurate scheme in time. The scheme is easy to implement since it is explicit. We also avoid the approximation of the time derivative of nonlinear function only except for initial time. Most of the studies in the literature focus on the only convergence of the semi-discrete scheme, conservation properties and stability analysis. Our aim is to prove error analysis of the exponential

wave integrator sine pseudo-spectral method for the higher-order Boussinesq equation involving the higher-order effects of dispersion. We obtain optimal error estimates of the fully-discrete scheme in the Sobolev space $H^m$.

## 2. PRELIMINARIES

In this section, we start introducing some notations and propositions employed throughout the thesis.

### 2.1 Discretization

$M$ and $N$ being positive integers, let us divide the interval $[a,b]$ into $M$ equal sub-intervals with grid spacing $h = (b-a)/M$ and the interval $[0,T]$ into $N$ equal sub-intervals with time step $\tau = T/N$. The spatial grid points are $x_j = a + jh$, $j = 0,1,2,\ldots,M$ and temporal grid points $t_n = n\tau,\ n = 0,\ldots,N$. Denote

$$X_M := \{u = (u_0,u_1,\ldots,u_M) \in \mathbb{R}^{M+1} | u_0 = u_M = 0\},$$
$$Y_M := \text{span}\{\sin(\mu_l(x-a)), \quad l = 1,2,\ldots,M-1\},$$

with $\mu_l = \frac{l\pi}{b-a}$.

### 2.2 Sine Transform

Let $u(x)$ be a general function on $\overline{\Omega} = [a,b]$ and $u \in X_M$. Define $P_M : L^2(\Omega) \to Y_M$ as the standard $L^2$-projection operator and $I_M : C_0(\overline{\Omega}) \to Y_M$ or $I_M : X_M \to Y_M$ as the trigonometric interpolation operator

$$(P_M u)(x) = \sum_{l=1}^{M-1} \widehat{u}_l \sin(\mu_l(x-a)), \qquad (I_M u)(x) = \sum_{l=1}^{M-1} \widetilde{u}_l \sin(\mu_l(x-a)), \tag{2.1}$$

where $\widehat{u}_l$ and $\widetilde{u}_l$ are the sine and discrete sine transform coefficients, respectively, given by

$$\widehat{u}_l = \frac{2}{b-a}\int_a^b u(x)\sin(\mu_l(x-a))dx, \qquad \widetilde{u}_l = \frac{2}{M}\sum_{j=1}^{M-1} u_j \sin\left(\frac{jl\pi}{M}\right), \tag{2.2}$$

with $u_j = u(x_j)$.

## 2.3 Sobolev Spaces

The following theory from [34] serves as a basis for the apprehension of the work to be presented.

Let $\Omega = (a,b)$ be a bounded interval of $\mathbb{R}$ and $L^2(\Omega)$ the space of the measurable functions $u : \Omega \to \mathbb{R}$ such that $\int_a^b |u(x)|dx < \infty$. The norm

$$\|u\|^2_{L^2(\Omega)} = \int_a^b |u(x)|^2 dx$$

is induced by the inner product

$$(u,v) = \int_a^b u(x)v(x)dx.$$

Let $m \geq 0$ be an integer. The Sobolev Space $H^m(\Omega)$ is defined as

$$H^m(\Omega) = \left\{ v \in L^2(\Omega) : \frac{d^k v}{dx^k} \in L^2(\Omega), 0 \leq k \leq m \right\}$$

with the inner product

$$(u,v)_m = \sum_{k=0}^{m} \int_a^b \frac{d^k u}{dx^k} \frac{d^k v}{dx^k} dx,$$

which induced the norm

$$\|u\|^2_{H^m(\Omega)} = \sum_{k=0}^{m} \left\| \frac{d^k u}{dx^k} \right\|^2_{L^2(\Omega)}.$$

Dirichlet conditions are one of the most generic boundary conditions related to a differential operator. Functions which satisfy the homogeneous Dirichlet boundary conditions that span the subspaces of the Sobolev spaces $H^m$ are significant. We know that the functions of $H^1(\Omega)$ are continuous up to the boundary by the Sobolev imbedding theorem. We introduce the following subspace of $H^1(\Omega)$:

$$H^1_0(\Omega) = \left\{ v \in H^1(\Omega) : v(a) = v(b) = 0 \right\}.$$

We define the subspace $H^m \cap H^1_0$ of the Sobolev space $H^m$ as

$$\widetilde{H}^m(\Omega) = \left\{ u \in H^m(\Omega) : u^{(2k)}(a) = u^{(2k)}(b) = 0, \quad k \in \mathbb{N}, \quad 0 \leq 2k < m \right\},$$

for some integer $m \geq 1$. For any function $u(x) = \sum_{l=1}^{\infty} \widehat{u}_l \sin(\mu_l(x-a)) \in \widetilde{H}^m(\Omega)$, the norm is defined as

$$\|u\|_m^2 = \sum_{l=1}^{\infty} \left(1 + |\mu_l|^2\right)^m |\widehat{u}_l|^2. \tag{2.3}$$

To attain the convergence of the fully discrete scheme, we need the following lemmas.

**Lemma 1.** *[26] For any $0 \leq \mu \leq k$ with $k > 1/2$, there exists a constant $C$ such that*

$$\|u - P_M u\|_\mu \leq C h^{k-\mu} \|u\|_k, \quad \|u - I_M u\|_\mu \leq C h^{k-\mu} \|u\|_k, \quad \forall u \in \widetilde{H}^k(\Omega). \tag{2.4}$$

**Lemma 2.** *[35] For $m > 1/2$, $H^m(\mathbb{R})$ is an algebra with respect to the product of functions. That is, if $u, v \in H^m(\mathbb{R})$ then $uv \in H^m(\mathbb{R})$ and*

$$\|uv\|_m \leq C \|u\|_m \|v\|_m. \tag{2.5}$$

**Lemma 3.** *[36] For any function $g \in C^\infty(\mathbb{C}, \mathbb{C})$ and $\sigma > 1/2$, there exists a nondecreasing function $\chi_g : \mathbb{R}^+ \to \mathbb{R}^+$ such that*

$$\|g(u)\|_\sigma \leq \|g(0)\|_\sigma + \chi_g(\|u\|_{L^\infty}) \|u\|_\sigma, \quad \forall u \in H^\sigma. \tag{2.6}$$

*For all $v, w \in B_R^\sigma := \{u \in H^\sigma : \|u\|_\sigma \leq R\}$, we have*

$$\|g(v) - g(w)\|_\sigma \leq \alpha(g, R) \|v - w\|_\sigma, \tag{2.7}$$

*where $\alpha(g, R) = \|g'(0)\|_\sigma + R\chi_{g'}(cR)$ is nondecreasing with respect to $R$, with $c > 0$ being the constant for the Sobolev imbedding $\|\cdot\|_{L^\infty} \leq c\|\cdot\|_\sigma$.*

**Young's Inequality.** *[37] For every $\varepsilon > 0$ and two non-negative numbers $a$ and $b$, the following inequality holds*

$$ab \leq \frac{\varepsilon a^2}{2} + \frac{b^2}{2\varepsilon},$$

*which gives*

$$(a+b)^2 \leq (1+\varepsilon)a^2 + \left(1 + \frac{1}{\varepsilon}\right) b^2.$$

**Discrete Gronwall's Lemma.** *[34] Let $u_n$ and $v_n$ be non-negative sequences satisfying*

$$u_{k+1} \leq \alpha + \sum_{n=0}^{k} u_n v_n$$

*for all n. Then for all n it holds*

$$u_{k+1} \leq \alpha \exp\left(\sum_{n=0}^{k} v_n\right).$$

Throughout this thesis, the notation $A \lesssim B$ is used to state that there exists a generic constant $C > 0$ such that $|A| \leq CB$. Here, $C$ does not depend on the time step $\tau$ or spatial step size $h$.

## 3. DERIVATION OF THE NUMERICAL METHOD

In this section, we solve the HBq equation by combining a sine pseudo-spectral method for spatial derivatives with the fourth-order exponential wave integrator for temporal derivatives. We consider the HBq equation on a bounded domain $\Omega = (a,b)$ with initial and homogeneous boundary conditions given by

$$\begin{cases} u_{tt} = u_{xx} + \eta_1 u_{xxtt} - \eta_2 u_{xxxxtt} + (f(u))_{xx}, \quad x \in \Omega, \quad t > 0, \\ u(x,0) = u_0(x), \quad u_t(x,0) = u_1(x), \\ u(a,t) = u(b,t) = 0, \quad t \geq 0, \end{cases} \tag{3.1}$$

where $f \in C^{\infty}(\mathbb{R},\mathbb{R})$. The space interval is chosen large enough so that the truncation error is negligible.

The sine pseudo-spectral approximation

$$u_M(x,t_n+s) = \sum_{l=1}^{M-1} \widehat{u}_l(t_n+s)\sin(\mu_l(x-a)), \qquad x \in \Omega, s \in \mathbb{R} \tag{3.2}$$

for the solution of (3.1) satisfies

$$\begin{aligned} \partial_{ss}u_M(x,t_n+s) &= \partial_{xx}u_M(x,t_n+s) + \eta_1\partial_{xxss}u_M(x,t_n+s) \\ &\quad -\eta_2\partial_{xxxxss}u_M(x,t_n+s) + \partial_{xx}P_M(f(u_M(x,t_n+s)). \end{aligned} \tag{3.3}$$

Substituting (3.2) into (3.3) and noticing the orthogonality of $\sin(\mu_l(x-a))$ for $l = 1,...,M-1$, one gets

$$\frac{d^2}{ds^2}\widehat{u}_l(t_n+s) + \theta_l^2\widehat{u}_l(t_n+s) + \theta_l^2(\widehat{f_M^n})_l(s) = 0, \qquad s \in \mathbb{R} \tag{3.4}$$

where $f_M^n(x,s) = P_M f(u_M(x,t_n+s))$ and $\theta_l = \mu_l/\sqrt{1+\eta_1\mu_l^2+\eta_2\mu_l^4}$.

By using the well-known variation of the parameters formula, the general solution of the equation (3.4) is given by

$$\begin{aligned} \widehat{u}_l(t_n+s) &= \cos(\theta_l s)\widehat{u}_l(t_n) + \frac{\sin(\theta_l s)}{\theta_l}\widehat{u}_l'(t_n) \\ &\quad -\theta_l\int_0^s \sin\big(\theta_l(s-\omega)\big)(\widehat{f_M^n})_l(\omega)d\omega. \end{aligned} \tag{3.5}$$

Differentiating (3.5) with respect to $s$, we obtain

$$\begin{aligned}\widehat{u}_l'(t_n+s) &= -\theta_l \sin(\theta_l s)\widehat{u}_l(t_n)+\cos(\theta_l s)\widehat{u}_l'(t_n)\\ &\quad -\theta_l^2\int_0^s \cos\big(\theta_l(s-\omega)\big)\widehat{(f_M^n)}_l(\omega)d\omega. \end{aligned} \tag{3.6}$$

Plugging $s=2\tau$ and replacing $n$ by $n-1$, one gets

$$\begin{aligned}\widehat{u}_l(t_{n+1}) &= \cos(2\theta_l\tau)\widehat{u}_l(t_{n-1})+\frac{\sin(2\theta_l\tau)}{\theta_l}\widehat{u}_l'(t_{n-1})\\ &\quad -\theta_l\int_0^{2\tau}\sin\big(\theta_l(2\tau-\omega)\big)\widehat{(f_M^{n-1})}_l(\omega)d\omega. \end{aligned} \tag{3.7}$$

In order to obtain the fourth-order accuracy method, we approximate the integral term in (3.7) by the Simpson rule as

$$\begin{aligned}\int_0^{2\tau}\sin\big(\theta_l(2\tau-\omega)\big)\widehat{(f_M^{n-1})}_l(\omega)d\omega &\approx \frac{\tau}{3}\Big[\sin(2\theta_l\tau)\widehat{(f_M^{n-1})}_l(0)\\ &\quad +4\sin(\theta_l\tau)\widehat{(f_M^n)}_l(0)\Big] \end{aligned} \tag{3.8}$$

noticing that $\widehat{(f_M^{n-1})}_l(\tau)=\widehat{(f_M^n)}_l(0)$. Similarly, plugging $s=2\tau$ and replacing $n$ by $n-1$ in (3.6), we obtain

$$\begin{aligned}\widehat{u}_l'(t_{n+1}) &= -\theta_l\sin(2\theta_l\tau)\widehat{u}_l(t_{n-1})+\cos(\theta_l s)\widehat{u}_l'(t_{n-1})\\ &\quad -\theta_l^2\int_0^{2\tau}\cos(\theta_l(2\tau-\omega))\widehat{(f_M^{n-1})}_l(w)d\omega. \end{aligned} \tag{3.9}$$

Applying Simpson's rule for approximating the integration in (3.9) yields

$$\begin{aligned}\int_0^{2\tau}\cos\big(\theta_l(2\tau-\omega)\big)\widehat{(f_M^{n-1})}_l(\omega)d\omega &\approx \frac{\tau}{3}\Big[\cos(2\theta_l\tau)\widehat{(f_M^{n-1})}_l(0)\\ &\quad +4\cos(\theta_l\tau)\widehat{(f_M^n)}_l(0)+\widehat{(f_M^{n+1})}_l(0)\Big]. \end{aligned} \tag{3.10}$$

In practice, computing the continuous sine coefficients in (3.7)-(3.10) is difficult. Therefore, we replace the continuous sine coefficients with the discrete sine coefficients as in (2.1) and (2.2). Now, we introduce the fourth-order EWI-SP scheme: Let $u_j^n$ and $\dot{u}_j^n (j=0,1,\ldots,M, n=0,1,\ldots)$ be the approximations to $u(x_j,t_n)$ and $u_t(x_j,t_n)$, respectively. Setting $u_j^0=u_0(x_j)$, $\dot{u}_j^0=u_1(x_j)$, the numerical approximations $u^{n+1},\dot{u}^{n+1}\in X_M$ are computed as

$$u_j^{n+1}=\sum_{l=1}^{M-1}\widetilde{u_l^{n+1}}\sin\left(\frac{jl\pi}{M}\right),\quad \dot{u}_j^{n+1}=\sum_{l=1}^{M-1}\widetilde{\dot{u}_l^{n+1}}\sin\left(\frac{jl\pi}{M}\right), \tag{3.11}$$

where the discrete sine coefficients are computed as follows for $n \geq 1$ :

$$\begin{aligned}
\widetilde{u_l^{n+1}} &= \cos(2\theta_l\tau)\widetilde{u_l^{n-1}} + \frac{\sin(2\theta_l\tau)}{\theta_l}\widetilde{\dot{u}_l^{n-1}} \\
&\quad -\frac{\theta_l\tau}{3}\Big[\sin(2\theta_l\tau)\widetilde{f_l^{n-1}} + 4\sin(\theta_l\tau)\widetilde{f_l^n}\Big], \\
\widetilde{\dot{u}_l^{n+1}} &= -\theta_l\sin(2\theta_l\tau)\widetilde{u_l^{n-1}} + \cos(2\theta_l\tau)\widetilde{\dot{u}_l^{n-1}} \\
&\quad -\frac{\theta_l^2\tau}{3}\Big[\cos(2\theta_l\tau)\widetilde{f_l^{n-1}} + 4\cos(\theta_l\tau)\widetilde{f_l^n} + \widetilde{f_l^{n+1}}\Big],
\end{aligned} \tag{3.12}$$

with

$$\begin{aligned}
\widetilde{u_l^n} &= \frac{2}{M}\sum_{j=1}^{M-1} u_j^n \sin\left(\frac{jl\pi}{M}\right), \qquad \widetilde{\dot{u}_l^n} = \frac{2}{M}\sum_{j=1}^{M-1} \dot{u}_j^n \sin\left(\frac{jl\pi}{M}\right), \\
\widetilde{f_l^n} &= \frac{2}{M}\sum_{j=1}^{M-1} f(u_j^n)\sin\left(\frac{jl\pi}{M}\right).
\end{aligned} \tag{3.13}$$

In order to start the iteration, we need the initial values $u^1$ and $\dot{u}^1$.

***Computation of*** $\widehat{u}_l(t_1)$: If we differentiate the equation (3.4) with respect to $s$, we obtain

$$\frac{d^3}{ds^3}\widehat{u}_l(t_n+s) + \theta_l^2\frac{d}{ds}\widehat{u}_l(t_n+s) + \theta_l^2\frac{d}{ds}\widehat{(f_M^n)}_l(s) = 0, \qquad s \in \mathbb{R}. \tag{3.14}$$

By using the equations (3.4) and (3.14) in Taylor's expansion, the fourth-order approximation can be written as

$$\begin{aligned}
\widehat{u}_l(t_1) &= \widehat{u}_l(0) + \tau\widehat{u}_l'(0) - \frac{\theta_l^2\tau^2}{2}\Big[\widehat{u}_l(0) + \widehat{(f_M^0)_l}(0)\Big] \\
&\quad -\frac{\theta_l^2\tau^3}{6}\Big[\widehat{u}_l'(0) + \widehat{(f_M^0)}_l'(0)\Big] + \frac{\tau^4}{24}\widehat{u}_l''''(s_{l,1}),
\end{aligned} \tag{3.15}$$

where $s_{l,1} \in (0,\tau)$. Since $f \in C^\infty(\mathbb{R},\mathbb{R})$, the sine coefficients $\widehat{(f_M^0)}_l'(0)$ for $l = 0,1,\ldots M-1$ are computed as

$$\widehat{(f_M^0)}_l'(0) = \Big[\widehat{f'\big(u_M(x,0)\big)\,\partial_s u_M(x,0)}\Big]_l. \tag{3.16}$$

***Computation of*** $\widehat{u}_l'(t_1)$: Approximating $\widehat{u}_l(t_0)$ and $\widehat{u}_l(t_2)$ by using Taylor's expansion around $t_1$, and taking their difference, one can get

$$\widehat{u}_l(t_2) - \widehat{u}_l(0) = 2\tau\widehat{u}_l'(t_1) + \frac{\tau^3}{3}\widehat{u}_l'''(t_1) + \frac{\tau^5}{60}\widehat{u}_l''''(s_{l,2}), \tag{3.17}$$

where $s_{l,2} \in (0, 2\tau)$. Using

$$\widehat{u}_l'''(t_1) = \frac{\widehat{u}_l''(t_2) - \widehat{u}_l''(0)}{2\tau} - \frac{\tau^2}{6}\widehat{u}_l''''(s_{l,3}), \tag{3.18}$$

where $s_{l,3} \in (0, 2\tau)$, the equation (3.17) becomes

$$\widehat{u}_l(t_2) - \widehat{u}_l(0) = 2\tau\widehat{u}_l'(t_1) + \frac{\tau^2}{6}\left[\widehat{u}_l''(t_2) - \widehat{u}_l''(0)\right] + \frac{\tau^5}{60}\widehat{u}_l''''(s_{l,2}) - \frac{\tau^5}{18}\widehat{u}_l''''(s_{l,3}). \tag{3.19}$$

By (3.4)

$$\widehat{u}_l''(t_2) - \widehat{u}_l''(0) = -\theta_l^2\left[\widehat{u}_l(t_2) - \widehat{u}_l(0) + \widehat{(f_M^2)}_l(0) - \widehat{(f_M^0)}_l(0)\right],$$

we obtain

$$\begin{aligned}\widehat{u}_l'(t_1) &= \left(\frac{1}{2\tau} + \frac{\theta_l^2\tau}{12}\right)\left[\widehat{u}_l(t_2) - \widehat{u}_l(0)\right] + \frac{\theta_l^2\tau}{12}\left[\widehat{(f_M^2)}_l(0) - \widehat{(f_M^0)}_l(0)\right] \\ &\quad + \frac{7\tau^4}{360}\widehat{u}_l''''(s_{l,4}),\end{aligned} \tag{3.20}$$

where $s_{l,4} \in (0, 2\tau)$.

By replacing the continuous sine coefficients with the discrete sine coefficients, the discrete sine coefficients at the first time step are obtained as follows:

$$\begin{aligned}\widetilde{u}_l^1 &= \widetilde{u}_l^0 + \tau\widetilde{\dot{u}}_l^0 - \frac{\theta_l^2\tau^2}{2}\left[\widetilde{u}_l^0 + \widetilde{f}_l^0\right] - \frac{\theta_l^2\tau^3}{6}\left[\widetilde{\dot{u}}_l^0 + \widetilde{\dot{f}}_l^0\right], \\ \widetilde{\dot{u}}_l^1 &= \left(\frac{1}{2\tau} + \frac{\theta_l^2\tau}{12}\right)\left(\widetilde{u}_l^2 - \widetilde{u}_l^0\right) + \frac{\theta_l^2\tau}{12}\left(\widetilde{f}_l^2 - \widetilde{f}_l^0\right),\end{aligned} \tag{3.21}$$

where

$$\widetilde{\dot{f}}_l^0 = \frac{2}{M}\sum_{j=1}^{M-1}\left[f'(u_j^0)\dot{u}_j^0\right]\sin\left(\frac{jl\pi}{M}\right). \tag{3.22}$$

To summarize, the scheme is based on the following steps:

*Step 1:* The discrete sine coefficients $\widetilde{u}_l^0$, $\widetilde{\dot{u}}_l^0$, $\widetilde{f}_l^0$, $\widetilde{\dot{f}}_l^0$ are found by using the formulas (3.13) and (3.22).

*Step 2:* $\widetilde{u}_l^1$ is computed by using (3.21).

*Step 3:* $\widetilde{f}_l^1$ is calculated by using (3.13) after constructing the approximate solution $u^1$.

*Step 4:* $\widetilde{u}_l^2$ is evaluated by using (3.12).

*Step 5:* $\widetilde{f_l^2}$ is obtained by using (3.13) after constructing the approximate solution $u^2$.

*Step 6:* $\widetilde{\dot{u}_l^1}$ and $\widetilde{\dot{u}_l^2}$ are evaluated by using (3.21) and (3.12), respectively, and then $\dot{u}^1$ and $\dot{u}^2$ are constructed.

*Step 7:* $u^n$ and $\dot{u}^n$ can be found for $n \geq 3$ by using (3.11)-(3.13).

## 4. ERROR ESTIMATE OF THE EXPONENTIAL WAVE INTEGRATOR METHOD FOR THE HIGHER ORDER BOUSSINESQ EQUATION

In this section, the error analysis for the fully discretized scheme (3.12) and (3.21) is presented. For simplicity of notation, the interpolations of the numerical solutions are given by

$$u_I^n(x) = I_M(u^n)(x), \quad \dot{u}_I^n(x) = I_M(\dot{u}^n)(x), \quad x \in (a,b),$$

and the error functions by

$$e^n(x) = u(x,t_n) - u_I^n(x), \quad \dot{e}^n(x) = \partial_t u(x,t_n) - \dot{u}_I^n(x), \quad x \in (a,b).$$

**Theorem 1.** *Let the solution of the HBq equation* (3.1) *satisfy the regularity properties* $u \in C^1\left([0,T];\widetilde{H}^{m+\sigma}\right) \cap C^5\left([0,T];\widetilde{H}^m\right)(m > \frac{1}{2}, \sigma > 0)$. *Then there exist* $h_0 > 0$ *and* $0 < \tau_0 \leq 1$ *such that when* $\tau \leq \tau_0$ *and* $h \leq h_0$, *the numerical solutions* $u^n$ *and* $\dot{u}^n$ *obtained from the EWI-SP scheme* (3.11)-(3.13) *with* (3.21) *and* (3.22) *converge to the solution of the problem* (3.1) *with the convergence rate*

$$\|e^n\|_m + \|\dot{e}^n\|_m \lesssim \tau^4 + h^\sigma, \qquad n = 0,1,\ldots,N, \tag{4.1}$$

*with* $\|\partial_t^k u\|_{L^\infty([0,T];H^m)} \leq K_k$ *for* $(k = 0,1,\ldots,5)$ *and* $\|\partial_t^k u\|_{L^\infty([0,T];H^{m+\sigma})} \leq R_k$ *for* $(k = 0,1)$. *Furthermore, we have*

$$\|u_I^n\|_m \leq K_0 + 1, \quad \|\dot{u}_I^n\|_m \leq K_1 + 1. \tag{4.2}$$

*Proof.* (4.1) and (4.2) are proved by mathematical induction. For $n = 0$, noticing that $e^0 = u_0 - I_M(u_0)$, $\dot{e}^0 = u_1 - I_M(u_1)$, applying Lemma 1, one gets

$$\|e^0\|_m + \|\dot{e}^0\|_m \lesssim h^\sigma. \tag{4.3}$$

There exists a constant $h_1 > 0$ such that, when $0 < h \leq h_1$, the inequality (4.2) is valid for $n = 0$. Assuming (4.1) and (4.2) are true for $n \leq k < T/\tau$, we show that (4.1) and

(4.2) are valid for $n = k+1$. The projected error functions are introduced by

$$e_M^n(x) = P_M(e^n(x)) = \sum_{l=1}^{M-1} \widehat{e_l^n} \sin(\mu_l(x-a)),$$
$$\dot{e}_M^n(x) = P_M(\dot{e}^n(x)) = \sum_{l=1}^{M-1} \widehat{\dot{e}_l^n} \sin(\mu_l(x-a)),$$

where the corresponding coefficients in the frequency satisfy

$$\widehat{e_l^n} = \widehat{u}_l(t_n) - \widetilde{u_l^n}, \qquad \widehat{\dot{e}_l^n} = \widehat{u}_l'(t_n) - \widetilde{\dot{u}_l^n}.$$

We define the local truncation errors

$$\xi^n(x) = \sum_{l=1}^{M-1} \widehat{\xi_l^n} \sin(\mu_l(x-a)), \qquad \dot{\xi}^n(x) = \sum_{l=1}^{M-1} \widehat{\dot{\xi}_l^n} \sin(\mu_l(x-a)),$$

where

$$\begin{aligned}
\widehat{\xi_l^n} &= \widehat{u}_l(t_{n+1}) - \cos(2\theta_l\tau)\widehat{u}_l(t_{n-1}) - \frac{\sin(2\theta_l\tau)}{\theta_l}\widehat{u}_l'(t_{n-1}) \\
&\quad + \frac{\theta_l\tau}{3}\Big[\sin(2\theta_l\tau)\widehat{f_l^{n-1}}(0) + 4\sin(\theta_l\tau)\widehat{f_l^n}(0)\Big], \\
\widehat{\dot{\xi}_l^n} &= \widehat{u}_l'(t_{n+1}) + \theta_l\sin(2\theta_l\tau)\widehat{u}_l(t_{n-1}) - \cos(2\theta_l\tau)\widehat{u}_l'(t_{n-1}) \\
&\quad + \frac{\theta_l^2\tau}{3}\Big[\cos(2\theta_l\tau)\widehat{f_l^{n-1}}(0) + 4\cos(\theta_l\tau)\widehat{f_l^n}(0) + \widehat{f_l^{n+1}}(0)\Big],
\end{aligned} \tag{4.4}$$

for $n \geq 1$ and

$$\begin{aligned}
\widehat{\xi_l^0} &= \widehat{u}_l(t_1) - \widehat{u}_l(0) - \tau\widehat{u}_l'(0) + \frac{\theta_l^2\tau^2}{2}\Big[\widehat{u}_l(0) + \widehat{f_l^0}(0)\Big] \\
&\quad + \frac{\theta_l^2\tau^3}{6}\Big[\widehat{u}_l'(0) + \widehat{(f_l^0)}'(0)\Big], \\
\widehat{\dot{\xi}_l^0} &= \widehat{u}_l'(t_1) - \Big(\frac{1}{2\tau} + \frac{\theta_l^2\tau}{12}\Big)\Big[\widehat{u}_l(t_2) - \widehat{u}_l(0)\Big] - \frac{\theta_l^2\tau}{12}\Big[\widehat{f_l^2}(0) - \widehat{f_l^0}(0)\Big],
\end{aligned} \tag{4.5}$$

with $\widehat{f_l^n}(s) = f(\widehat{u(t_n+s)})_l$.

If we subtract the equations (3.12) and (3.21) from the equations (4.4) and (4.5) respectively, the resulting error equations for $n \geq 1$ become

$$\begin{aligned}
\widehat{e_l^{n+1}} &= \cos(2\theta_l\tau)\widehat{e_l^{n-1}} + \frac{\sin(2\theta_l\tau)}{\theta_l}\widehat{\dot{e}_l^{n-1}} + \widehat{\xi_l^n} \\
&\quad -\frac{\theta_l\tau}{3}\Big[\sin(2\theta_l\tau)\widehat{\eta_l^{n-1}} + 4\sin(\theta_l\tau)\widehat{\eta_l^n}\Big] \qquad (4.6)\\
\widehat{\dot{e}_l^{n+1}} &= -\theta_l\sin(2\theta_l\tau)\widehat{e_l^{n-1}} + \cos(2\theta_l\tau)\widehat{\dot{e}_l^{n-1}} + \widehat{\dot{\xi}_l^n} \\
&\quad -\frac{\theta_l^2\tau}{3}\Big[\cos(2\theta_l\tau)\widehat{\eta_l^{n-1}} + 4\cos(\theta_l\tau)\widehat{\eta_l^n} + \widehat{\eta_l^{n+1}}\Big]. \qquad (4.7)
\end{aligned}$$

and

$$\begin{aligned}
\widehat{e_l^1} &= \widehat{e_l^0} + \tau\widehat{\dot{e}_l^0} + \widehat{\xi_l^0} - \frac{\theta_l^2\tau^2}{2}\Big[\widehat{e_l^0} + \widehat{\eta_l^0}\Big] - \frac{\theta_l^2\tau^3}{2}\Big[\widehat{\dot{e}_l^0} + \widehat{\dot{\eta}_l^0}\Big], \qquad (4.8)\\
\widehat{\dot{e}_l^1} &= \Big(\frac{1}{2\tau} + \frac{\theta_l^2\tau}{12}\Big)\Big(\widehat{e_l^2} - \widehat{e_l^0}\Big) + \widehat{\dot{\xi}_l^0} + \frac{\theta_l^2\tau}{12}\Big[\widehat{\eta_l^2} - \widehat{\eta_l^0}\Big], \qquad (4.9)
\end{aligned}$$

where the nonlinear errors are

$$\eta^n(x) = \sum_{l=1}^{M-1}\widehat{\eta_l^n}\sin(\mu_l(x-a)), \qquad \dot{\eta}^0(x) = \sum_{l=1}^{M-1}\widehat{\dot{\eta}_l^0}\sin(\mu_l(x-a))$$

with $\widehat{\eta_l^n} = \widehat{f_l^n}(0) - \widetilde{f_l^n}$ and $\widehat{\dot{\eta}_l^0} = \widehat{(f_l^0)'}(0) - \widetilde{\dot{f}_l^0}$.

***Step 1***: Estimation of Local Truncation Errors

Substituting (3.7) and (3.9) into (4.4), (3.15) and (3.20) into (4.5) respectively, the resulting truncation errors for $n \geq 1$ become

$$\begin{aligned}
\widehat{\xi_l^n} &= -\theta_l\int_0^{2\tau}\sin\big(\theta_l(2\tau-\omega)\big)\widehat{f_l^{n-1}}(\omega)d\omega \\
&\quad +\frac{\theta_l\tau}{3}\Big[\sin(2\theta_l\tau)\widehat{f_l^{n-1}}(0) + 4\sin(\theta_l\tau)\widehat{f_l^n}(0)\Big], \\
\widehat{\dot{\xi}_l^n} &= -\theta_l^2\int_0^{2\tau}\cos\big(\theta_l(2\tau-\omega)\big)\widehat{f_l^{n-1}}(\omega)d\omega \\
&\quad +\frac{\theta_l^2\tau}{3}\Big[\cos(2\theta_l\tau)\widehat{f_l^{n-1}}(0) + 4\cos(\theta_l\tau)\widehat{f_l^n}(0) + \widehat{f_l^{n+1}}(0)\Big]
\end{aligned} \qquad (4.10)$$

and

$$\widehat{\xi_l^0} = \frac{\tau^4}{24}\widehat{u}_l''''(s_{l,1}), \qquad \widehat{\dot{\xi}_l^0} = \frac{7\tau^4}{360}\widehat{u}_l''''(s_{l,4}).$$

It is clear that

$$\|\xi^0\|_m^2 + \|\dot{\xi}^0\|_m^2 \lesssim \tau^8. \qquad (4.11)$$

The local truncation errors in (4.10) actually come from the error using the Simpson rule. Using the standard error formula of the Simpson rule for a general function $v(s) \in C^4[0,2\tau]$

$$\int_0^{2\tau} v(s)ds - \frac{\tau}{3}\big[v(0)+4v(\tau)+v(2\tau)\big] = -\frac{8\tau^5}{45}v^{(4)}(c), \qquad c \in (0,2\tau),$$

the local truncation errors (4.10) become

$$\begin{aligned}
\widehat{\xi_l^n} &= \frac{8\theta_l}{45}\tau^5\left(\frac{d^4}{d\omega^4}\Big[\sin\big(\theta_l(2\tau-\omega)\big)\widehat{(f_l^{n-1})}(\omega)\Big]\Big|_{\omega=s_{l,5}}\right)\\
&= \frac{8\theta_l}{45}\tau^5\Big[\theta_l^4\sin\big(\theta_l(2\tau-s_{l,5})\big)\widehat{f}_l^{n-1}(s_{l,5})\\
&\quad +4\theta_l^3\cos\big(\theta_l(2\tau-s_{l,5})\big)\widehat{(f_l^{n-1})}'(s_{l,5})\\
&\quad -6\theta_l^2\sin\big(\theta_l(2\tau-s_{l,5})\big)\widehat{(f_l^{n-1})}''(s_{l,5})\\
&\quad -4\theta_l\cos\big(\theta_l(2\tau-s_{l,5})\big)\widehat{(f_l^{n-1})}'''(s_{l,5})\\
&\quad +\sin\big(\theta_l(2\tau-s_{l,5})\big)\widehat{(f_l^{n-1})}''''(s_{l,5})\Big],\\
\widehat{\dot{\xi}_l^n} &= \frac{8\theta_l^2}{45}\tau^5\left(\frac{d^4}{d\omega^4}\Big[\cos\big(\theta_l(2\tau-\omega)\big)\widehat{(f_l^{n-1})}(\omega)\Big]\Big|_{\omega=s_{l,6}}\right)\\
&= \frac{8\theta_l^2}{45}\tau^5\Big[\theta_l^4\cos\big(\theta_l(2\tau-s_{l,6})\big)\widehat{f}_l^{n-1}(s_{l,6})\\
&\quad -4\theta_l^3\sin\big(\theta_l(2\tau-s_{l,6})\big)\widehat{(f_l^{n-1})}'(s_{l,6})\\
&\quad -6\theta_l^2\cos\big(\theta_l(2\tau-s_{l,6})\big)\widehat{(f_l^{n-1})}''(s_{l,6})\\
&\quad +4\theta_l\sin\big(\theta_l(2\tau-s_{l,6})\big)\widehat{(f_l^{n-1})}'''(s_{l,6})\\
&\quad +\cos\big(\theta_l(2\tau-s_{l,6})\big)\widehat{(f_l^{n-1})}''''(s_{l,6})\Big]
\end{aligned}$$

where $s_{l,5}, s_{l,6} \in (0,2\tau)$. Since $\eta_1$ and $\eta_2$ are positive real numbers, we have $|\theta_l| \le 1/\sqrt{\eta_1}$. Applying Young's inequality to the above equations, we deduce

$$\begin{aligned}
|\widehat{\xi_l^n}|^2 &\le C\tau^{10}\Big[|\widehat{f}_l^{n-1}(s_{l,5})|^2+|\widehat{(f_l^{n-1})}'(s_{l,5})|^2+|\widehat{(f_l^{n-1})}''(s_{l,5})|^2\\
&\quad +|\widehat{(f_l^{n-1})}'''(s_{l,5})|^2+|\widehat{(f_l^{n-1})}''''(s_{l,5})|^2\Big],\\
|\widehat{\dot{\xi}_l^n}|^2 &\le C\tau^{10}\Big[|\widehat{f}_l^{n-1}(s_{l,6})|^2+|\widehat{(f_l^{n-1})}'(s_{l,6})|^2+|\widehat{(f_l^{n-1})}''(s_{l,6})|^2\\
&\quad +|\widehat{(f_l^{n-1})}'''(s_{l,6})|^2+|\widehat{(f_l^{n-1})}''''(s_{l,6})|^2\Big].
\end{aligned}$$

Using the assumptions $\|\partial_t^k u\|_{L^\infty([0,T];H^m)} \le K_k$ for $(k=0,1,\ldots,4)$ and $f \in C^\infty(\mathbb{R},\mathbb{R})$, it follows that

$$\|\xi^n\|_m^2 + \|\dot{\xi}^n\|_m^2 \le C(f,K_0,K_1,K_2,K_3,K_4)\tau^{10} \lesssim \tau^{10} \tag{4.12}$$

for $n \ge 1$.

***Step 2***: Estimation of Nonlinear Errors

Now, we show that $\dot{\eta}^0$ and $\eta^n$ are bounded in $H^m$ with $m > 1/2$. We use Lemmas 1-3 and $u_I^n, u(\cdot,t_n) \in B_{K_0+1}^m$ to obtain

$$\begin{aligned}
\|\dot{\eta}^0\|_m &= \Big\| I_M\big(f'(u_I^0)\dot{u}_I^0\big) - P_M\big(f'(u(\cdot,0))\partial_t u(\cdot,0)\big)\Big\|_m \\
&\le \Big\| I_M\Big[f'(u_I^0)\dot{u}_I^0 - f'(u(\cdot,0))\dot{u}_I^0\Big]\Big\|_m \\
&\quad + \Big\| I_M\Big[f'(u(\cdot,0))\dot{u}_I^0 - f'(u(\cdot,0))\partial_t u(\cdot,0)\Big]\Big\|_m \\
&\quad + \Big\| I_M\big(f'(u(\cdot,0))\partial_t u(\cdot,0)\big) - P_M\big(f'(u(\cdot,0))\partial_t u(\cdot,0)\big)\Big\|_m, \\
&\le C\Big\| f'\big(u_I^0\big)\dot{u}_I^0 - f'\big(u(\cdot,0)\big)\dot{u}_I^0\Big\|_m \\
&\quad + C\Big\| f'\big(u(\cdot,0)\big)\dot{u}_I^0 - f'\big(u(\cdot,0)\big)\partial_t u(\cdot,0)\Big\|_m \\
&\quad + Ch^\sigma\Big\| f'\big(u(\cdot,0)\big)\partial_t u(\cdot,0)\Big\|_{m+\sigma} \\
&\le C\|\dot{u}_I^0\|_m\Big\| f'\big(u_I^0\big) - f'\big(u(\cdot,0)\big)\Big\|_m \\
&\quad + C\Big\| f'\big(u(\cdot,0)\big)\Big\|_m\Big\|\dot{u}_I^0 - \partial_t u(\cdot,0)\Big\|_m \\
&\quad + Ch^\sigma\Big\| f'\big(u(\cdot,0)\big)\Big\|_{m+\sigma}\Big\|\partial_t u(\cdot,0)\Big\|_{m+\sigma} \\
&\le C\alpha\Big(f', K_0+1\Big)\|\dot{u}_I^0\|_m\|u_I^0 - u(\cdot,0)\|_m \\
&\quad + C\Big[\|f'(0)\|_m + \chi_{f'}\big(\|u(\cdot,0)\|_{L^\infty}\big)\|u(\cdot,0)\|_m\Big]\|\dot{u}_I^0 - \partial_t u(\cdot,0)\|_m \\
&\quad + Ch^\sigma\Big[\|f'(0)\|_{m+\sigma} \\
&\quad + \chi_{f'}\big(\|u(\cdot,0)\|_{L^\infty}\big)\|u(\cdot,0)\|_{m+\sigma}\Big]\|\partial_t u(\cdot,0)\|_{m+\sigma} \\
&\le C\alpha\Big(f', K_0+1\Big)\|\dot{u}_I^0\|_m\|e_M^0\|_m \\
&\quad + C\Big[\|f'(0)\|_m + \chi_{f'}(cK_0)K_0\Big]\|\dot{e}_M^0\|_m \\
&\quad + Ch^\sigma\Big[\|f'(0)\|_{m+\sigma} + \chi_{f'}(cR_0)R_0\Big]R_1, \\
&\le C(f,K_0)\big(\|e_M^0\|_m + \|\dot{e}_M^0\|_m\big) + C(f,R_0,R_1)h^\sigma.
\end{aligned} \tag{4.13}$$

On the other hand,

$$\begin{aligned}
\|\eta^n\|_m &= \Big\|I_M\big(f(u_I^n)\big) - P_M\big(f(u(\cdot,t_n))\big)\Big\|_m \\
&\le \Big\|I_M\Big[f(u_I^n) - f(u(\cdot,t_n))\Big]\Big\|_m \\
&\quad + \Big\|I_M\big(f(u(\cdot,t_n))\big) - P_M\big(f(u(\cdot,t_n))\big)\Big\|_m \\
&\le C\Big\|f\big(u_I^n\big) - f\big(u(\cdot,t_n)\big)\Big\|_m + Ch^\sigma\Big\|f\big(u(\cdot,t_n)\big)\Big\|_{m+\sigma} \\
&\le C\alpha\Big(f, K_0+1\Big)\|u_I^n - u(\cdot,t_n)\|_m + Ch^\sigma\Big(\|f(0)\|_{m+\sigma} \\
&\quad + \chi_f\big(\|u(\cdot,t_n)\|_{L^\infty}\big)\|u(\cdot,t_n)\|_{m+\sigma}\Big) \\
&\le C\alpha\Big(f, K_0+1\Big)\|e_M^n\|_m + C(f,R_0)h^\sigma.
\end{aligned}$$

In order to estimate $\|\eta^{n+1}\|_m$, we need to find an upper bound for $\|u_I^{n+1}\|_m$. It follows that

$$\begin{aligned}
\|u_I^{n+1}\|_m &\le \|u_I^{n-1}\|_m + 2\tau\|\dot{u}_I^{n-1}\|_m \\
&\quad + C\tau\Big(\|I_M(f(u_I^{n-1}))\|_m + \|I_M(f(u_I^n))\|_m\Big) \\
&\le K_0 + 2\tau K_1 + C\tau\Big(\|f(u_I^{n-1})\|_m + \|f(u_I^n)\|_m\Big) \\
&\le K_0 + 2\tau K_1 + C\tau\Big(2\|f(0)\|_m + \chi_f(c\|u_I^{n-1}\|_m)\|u_I^{n-1}\|_m \\
&\quad + \chi_f(c\|u_I^n\|_m)\|u_I^n\|_m\Big) \\
&\le C(f, K_0, K_1).
\end{aligned}$$

Therefore, we deduce that

$$\|\eta^{n+1}\|_m \lesssim \|e_M^{n+1}\|_m + h^\sigma. \tag{4.14}$$

***Step 3***: Error Equations

From the equation (4.8), one gets

$$\begin{aligned}
|\widehat{e_l^1}|^2 &\lesssim (1+\tau^2+\tau^4)|\widehat{e_l^0}|^2 + (\tau^2+\tau^4+\tau^6)|\widehat{\dot{e}_l^0}|^2 + |\widehat{\xi_l^0}|^2 + \tau^4|\widehat{\eta_l^0}|^2 \\
&\quad + \tau^6|\widehat{\dot{\eta}_l^0}|^2.
\end{aligned}$$

Substituting (4.6) with $n=1$ into (4.9) yields

$$\begin{aligned}\widehat{\dot{e}_l^1} &= \left(1+\frac{\theta_l^2\tau^2}{6}\right)\Bigg[-\left(\frac{1-\cos(2\theta_l\tau)}{2\theta_l\tau}\right)\theta_l\widehat{e_l^0}+\left(\frac{\sin(2\theta_l\tau)}{2\theta_l\tau}\right)\widehat{\dot{e}_l^0}\\ &\quad+\frac{1}{2\tau}\widehat{\xi_l^1}-\frac{\theta_l^2\tau}{3}\left(\frac{\sin(2\theta_l\tau)}{2\theta_l\tau}\right)\widehat{\eta_l^0}-\frac{2\theta_l^2\tau}{3}\left(\frac{\sin(\theta_l\tau)}{\theta_l\tau}\right)\widehat{\eta_l^1}\Bigg]\\ &\quad+\widehat{\dot{\xi}_l^0}+\frac{\theta_l^2\tau}{12}\Big[\widehat{\eta_l^2}-\widehat{\eta_l^0}\Big].\end{aligned}$$

This implies that

$$\begin{aligned}|\widehat{\dot{e}_l^1}|^2 &\lesssim (1+\tau^2+\tau^4)\big(\theta_l^2|\widehat{e_l^0}|^2+|\widehat{\dot{e}_l^0}|^2\big)+|\widehat{\dot{\xi}_l^0}|^2+\Big(\frac{1}{\tau^2}+1+\tau^2\Big)|\widehat{\xi_l^1}|^2\\ &\quad+(\tau^2+\tau^4+\tau^6)|\widehat{\eta_l^0}|^2+(\tau^2+\tau^4+\tau^6)|\widehat{\eta_l^1}|^2+\tau^2|\widehat{\eta_l^2}|^2.\end{aligned}$$

Hence,

$$\begin{aligned}\theta_l^2|\widehat{e_l^1}|^2+|\widehat{\dot{e}_l^1}|^2 &\lesssim (1+\tau^2+\tau^4+\tau^6)\big(\theta_l^2|\widehat{e_l^0}|^2+|\widehat{\dot{e}_l^0}|^2\big)+|\widehat{\xi_l^0}|^2+|\widehat{\dot{\xi}_l^0}|^2\\ &\quad+\Big(\frac{1}{\tau^2}+1+\tau^2\Big)|\widehat{\xi_l^1}|^2+(\tau^2+\tau^4+\tau^6)|\widehat{\eta_l^0}|^2\\ &\quad+(\tau^2+\tau^4+\tau^6)|\widehat{\eta_l^1}|^2+\tau^2|\widehat{\eta_l^2}|^2+\tau^6|\widehat{\dot{\eta}_l^0}|^2\\ &\lesssim \big(\theta_l^2|\widehat{e_l^0}|^2+|\widehat{\dot{e}_l^0}|^2\big)+|\widehat{\xi_l^0}|^2+|\widehat{\dot{\xi}_l^0}|^2+\frac{1}{\tau^2}|\widehat{\xi_l^1}|^2\\ &\quad+\tau^2\big(|\widehat{\eta_l^0}|^2+|\widehat{\eta_l^1}|^2+|\widehat{\eta_l^2}|^2\big)+\tau^6|\widehat{\dot{\eta}_l^0}|^2\end{aligned}\tag{4.15}$$

for $\tau\le 1$. Applying the triangle and Young's inequalities to (4.6) and (4.7), we obtain

$$\begin{aligned}|\widehat{e_l^{n+1}}|^2 &\le (1+\tau)\frac{\big|\theta_l\cos(2\theta_l\tau)\widehat{e_l^{n-1}}+\sin(2\theta_l\tau)\widehat{\dot{e}_l^{n-1}}\big|^2}{\theta_l^2}\\ &\quad+C\left(1+\frac{1}{\tau}\right)\left[|\widehat{\xi_l^n}|^2+\tau^2\big(|\widehat{\eta_l^{n-1}}|^2+|\widehat{\eta_l^n}|^2\big)\right],\\ |\widehat{\dot{e}_l^{n+1}}|^2 &\le (1+\tau)\big|-\theta_l\sin(2\theta_l\tau)\widehat{e_l^{n-1}}+\cos(2\theta_l\tau)\widehat{\dot{e}_l^{n-1}}\big|^2\\ &\quad+C\left(1+\frac{1}{\tau}\right)\left[|\widehat{\dot{\xi}_l^n}|^2+\tau^2\big(|\widehat{\eta_l^{n-1}}|^2+|\widehat{\eta_l^n}|^2+|\widehat{\eta_l^{n+1}}|^2\big)\right]\end{aligned}$$

for $n\ge 1$. Hence,

$$\begin{aligned}\theta_l^2|\widehat{e_l^{n+1}}|^2+|\widehat{\dot{e}_l^{n+1}}|^2 &\le (1+\tau)\big(\theta_l^2|\widehat{e_l^{n-1}}|^2+|\widehat{\dot{e}_l^{n-1}}|^2\big)\\ &\quad+C\left(\frac{1}{\tau}+1\right)\big(|\widehat{\xi_l^n}|^2+|\widehat{\dot{\xi}_l^n}|^2\big)\\ &\quad+(\tau+\tau^2)\big(|\widehat{\eta_l^{n-1}}|^2+|\widehat{\eta_l^n}|^2+|\widehat{\eta_l^{n+1}}|^2\big).\end{aligned}\tag{4.16}$$

Moreover, we define

$$\mathscr{E}^n = \sum_{l=1}^{M-1} \big(1+|\mu_l|^2\big)^m \Big(\theta_l^2 |\widehat{e_l^n}|^2 + |\widehat{\dot{e}_l^n}|^2\Big). \tag{4.17}$$

It is easy to see that

$$\mathscr{E}^0 \lesssim \|e_M^0\|_m^2 + \|\dot{e}_M^0\|_m^2 \lesssim \|e^0\|_m^2 + \|\dot{e}^0\|_m^2 \lesssim h^{2\sigma}, \tag{4.18}$$

by Lemma 1 and equation (4.3). Combining the inequalities (4.11), (4.12) and

$$\|\dot{\eta}^0\|_m^2 \lesssim h^{2\sigma}, \qquad \|\eta^n\|_m^2 \lesssim \mathscr{E}^n + h^{2\sigma}, \tag{4.19}$$

one can estimate

$$\begin{aligned}
\mathscr{E}^1 &\lesssim \mathscr{E}^0 + \|\xi^0\|_m^2 + \|\dot{\xi}^0\|_m^2 + \frac{1}{\tau^2}\|\xi^1\|_m^2 \\
&\quad + \tau^2\big(\|\eta^0\|_m^2 + \|\eta^1\|_m^2 + \|\eta^2\|_m^2\big) + \tau^6\|\dot{\eta}^0\|_m^2 \\
&\lesssim \tau^8 + (1+\tau^2+\tau^6)h^{2\sigma} + \tau^2(\mathscr{E}^1 + \mathscr{E}^2) \\
&\lesssim \tau^8 + h^{2\sigma} + \tau^2\mathscr{E}^2.
\end{aligned} \tag{4.20}$$

for $0 < \tau \le \tau_1$. Using (4.16), we obtain

$$\begin{aligned}
\mathscr{E}^{n+1} &\le (1+\tau)\mathscr{E}^{n-1} + C\left(\frac{1}{\tau}+1\right)\big(\|\xi^n\|_m^2 + \|\dot{\xi}^n\|_m^2\big) \\
&\quad + (\tau+\tau^2)\big(\|\eta^{n-1}\|_m^2 + \|\eta^n\|_m^2 + \|\eta^{n+1}\|_m^2\big)
\end{aligned}$$

for $n \ge 1$. This implies that

$$\begin{aligned}
\mathscr{E}^{n+1} - \mathscr{E}^{n-1} &\lesssim \tau\mathscr{E}^{n-1} + \frac{1}{\tau}\big(\|\xi^n\|_m^2 + \|\dot{\xi}^n\|_m^2\big) \\
&\quad + \tau\big(\|\eta^{n-1}|_m^2 + \|\eta^n\|_m^2 + \|\eta^{n+1}\|_m^2\big).
\end{aligned} \tag{4.21}$$

Substituting (4.12) and (4.19) into (4.21), we get

$$\mathscr{E}^{n+1} - \mathscr{E}^{n-1} \lesssim \tau\big(\mathscr{E}^{n-1} + \mathscr{E}^n + \mathscr{E}^{n+1}\big) + \tau^9 + \tau h^{2\sigma}.$$

Summing the above inequalities from $n = 1$ to $n = k$ such that $k \le T/\tau$, one can find

$$\begin{aligned}
\mathscr{E}^{k+1} + \mathscr{E}^k - \mathscr{E}^1 - \mathscr{E}^0 &\lesssim k\tau^9 + k\tau h^{2\sigma} + \tau\sum_{n=0}^{k+1}\mathscr{E}^n \\
&\lesssim \tau^8 + h^{2\sigma} + \tau\sum_{n=0}^{k+1}\mathscr{E}^n.
\end{aligned}$$

In view of (4.18), (4.20), one may estimate

$$\begin{aligned}
\mathscr{E}^{k+1} &\lesssim \mathscr{E}^0+\mathscr{E}^1+\tau^8+h^{2\sigma}+\tau\sum_{n=0}^{k+1}\mathscr{E}^n-\mathscr{E}^k \\
&\lesssim \tau^8+h^{2\sigma}+\tau\sum_{n=0}^{k}\mathscr{E}^n+\tau^2\mathscr{E}^2+\tau\mathscr{E}^{k+1} \\
&\lesssim \tau^8+h^{2\sigma}+\tau\sum_{n=0}^{k}\mathscr{E}^n \qquad (4.22)
\end{aligned}$$

for $0<\tau\leq\tau_2$. When the discrete Gronwall's Lemma is applied to (4.22), we finally show that

$$\mathscr{E}^{k+1}\lesssim\left(\tau^8+h^{2\sigma}\right)\exp\Big(\sum_{n=0}^{k}\tau\Big)\lesssim\tau^8+h^{2\sigma}. \qquad (4.23)$$

Moreover, using Lemma 1 and the equation (4.23), we deduce that

$$\begin{aligned}
\|e^{k+1}\|_m+\|\dot{e}^{k+1}\|_m &\lesssim \|e_M^{k+1}\|_m+\left\|u(\cdot,t_{k+1})-P_M\big(u(\cdot,t_{k+1})\big)\right\|_m \\
&\quad +\|\dot{e}_M^{k+1}\|_m \\
&\quad +\left\|\partial_t u(\cdot,t_{k+1})-P_M\big(\partial_t u(\cdot,t_{k+1})\big)\right\|_m \\
&\lesssim \tau^4+h^{\sigma}.
\end{aligned}$$

There exist sufficiently small $h_2$ and $\tau_3$ such that the following inequalities hold

$$\begin{aligned}
\|u_I^{k+1}\|_m &\leq \|e_M^{k+1}\|_m+\|u(\cdot,t_{k+1})\|_m\leq K_0+1, \\
\|\dot{u}_I^{k+1}\|_m &\leq \|\dot{e}_M^{k+1}\|_m+\|\partial_t u(\cdot,t_{k+1})\|_m\leq K_1+1,
\end{aligned}$$

when $0<h\leq h_2$ and $0<\tau\leq\tau_3$. The proof of the Theorem 1 is completed by choosing $h_0=\min\{h_1,h_2\}$ and $\tau_0=\min\{1,\tau_1,\tau_2,\tau_3\}$. □

## 5. NUMERICAL EXPERIMENTS

To investigate the performance of the proposed EWI-SP method, we now consider the propagation of a single solitary wave, the single wave splitting, the head-on collision of two solitary waves. The nonlinear function $f(u) = u^p$ with $p = 2$ or $p = 3$ is chosen for all the numerical experiments. To quantify the error, we use the following error function

$$e_{\tau,h}(t_n) = \left\| u^n_{\tau,h} - u(\cdot,t_n) \right\|_1 + \left\| \dot{u}^n_{\tau,h} - \partial_t u(\cdot,t_n) \right\|_1,$$

where $u^n_{\tau,h}$ and $\dot{u}^n_{\tau,h}$ are the numerical solutions obtained by the EWI-SP method. We also examine the change in the conserved quantity (mass) given in [24] as

$$\mathscr{M}(t) = \int_{-\infty}^{\infty} v_t \, dx, \tag{5.1}$$

where $u = v_x$.

### 5.1 Single Solitary Wave

The exact solitary wave solution of the HBq equation is given in [24] as

$$u(x,t) = A\left[ \operatorname{sech}\left(B(x - ct - x_0)\right)\right]^{\frac{4}{p-1}}, \tag{5.2}$$

where

$$A = \left[\frac{\eta_1^2 c^2 (p+1)(p+3)(3p+1)}{2\eta_2 (p^2+2p+5)^2}\right]^{\frac{1}{p-1}}, \qquad B = \left[\frac{\eta_1 (p-1)^2}{4\eta_2 (p^2+2p+5)}\right]^{\frac{1}{2}}, \tag{5.3}$$

$$c^2 = \left(1 - \left[\frac{4\eta_1^2 (p+1)^2}{\eta_2 (p^2+2p+5)^2}\right]\right)^{-1}. \tag{5.4}$$

Here, $A$ is amplitude, $B$ is the inverse width of the solitary wave and $c$ represents the velocity of the solitary wave at $x_0$ with $c^2 > 1$.

The problem is solved on the space interval $\Omega = (-400, 400)$ for times up to $T = 10$. We choose the parameters $\eta_1 = \eta_2 = 1$ with $x_0 = 0$ taking the initial condition corresponding to the exact solitary wave solution in (5.2)-(5.4). To validate that the

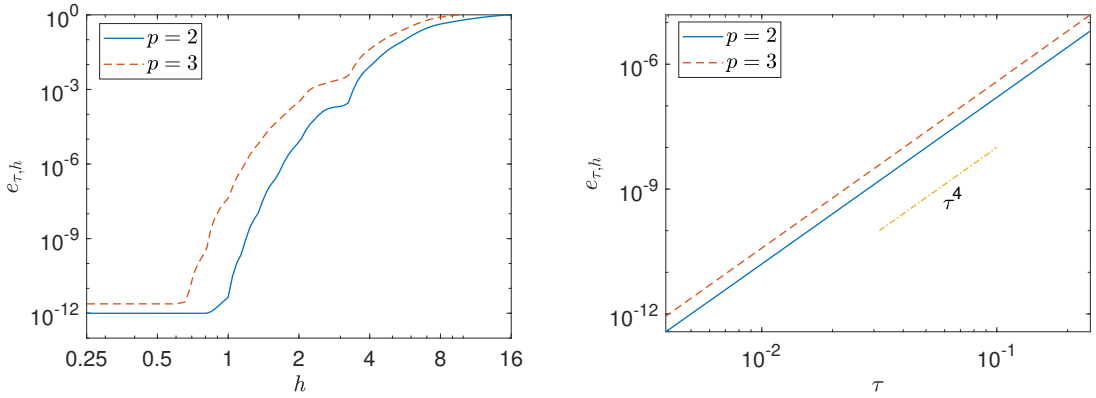


**Figure 5.1 :** The spatial errors (left panel) and the temporal errors (right panel) of the EWI-SP method for the solution under different grid spacing and time steps.

EWI-SP method yields the expected convergence rate in the space, some numerical experiments are performed for various values of step size $h$ and a fixed value of time step $\tau$. We take a tiny time step $\tau = 0.005$ so that the temporal error is negligible. In the left panel of Figure 5.1, we present the variation of the error with different values of $h$. As is seen from the figure, the error decays very rapidly when the spatial step size $h$ decreases. This numerical experiment shows that the EWI-SP method converges rapidly to the accurate solution in space, which is indicative of exponential convergence. In order to confirm the temporal error bound given in Theorem (1), the computations are performed for fixed value $h = 0.5$ and various values of the time step $\tau$. The right panel of Figure 5.1 shows the temporal errors of the EWI-SP method. As we expected, the scheme has fourth-order accuracy in time, which agrees with the theoretical result in Theorem 1.

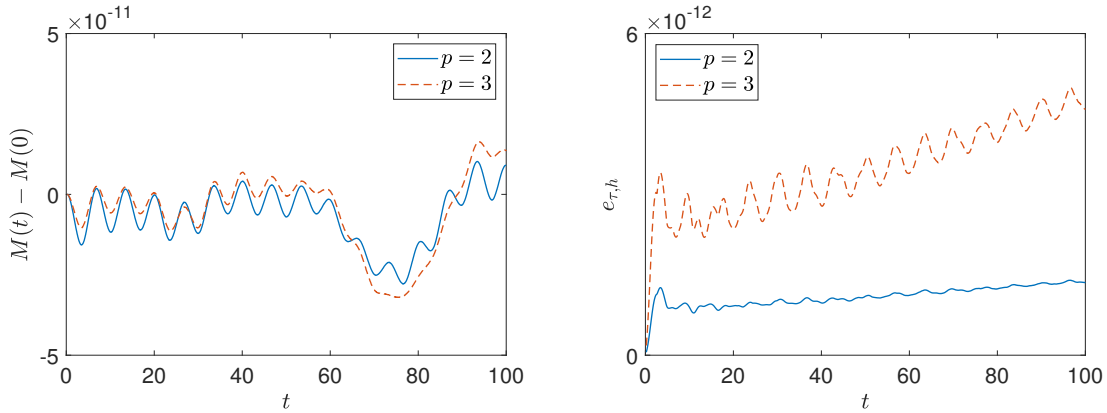


**Figure 5.2 :** Conservation of mass (left panel) and long-time errors (right panel) of the EWI-SP method by choosing $h = 0.5$ and $\tau = 0.005$

The evolution of the change for the conserved quantity $\mathscr{M}$ is depicted in the left panel of Figure 5.2. This figure illustrates that the EWI-SP method preserves conserved quantity very well. Next, we investigate the long-time behavior of the EWI-SP method up to $T = 100$. The right panel of Figure 5.2 shows that the error is about $10^{-12}$, even for the cubic nonlinearity. It can be observed that the EWI-SP method is reliable for long-time dynamics.

### 5.2 Single Wave Splitting

In these numerical experiments, we set $\eta_1 = \eta_2 = 1$. The initial data

$$u_0(x) = \frac{15}{38}\operatorname{sech}^4\left(\frac{\sqrt{13}}{26}x\right), \qquad u_1(x) = 0$$

are chosen for quadratic nonlinearity. We take the following initial data

$$u_0(x) = \sqrt{\frac{5}{14}}\operatorname{sech}^2\left(\frac{\sqrt{5}}{10}x\right), \qquad u_1(x) = 0$$

for cubic nonlinearity.

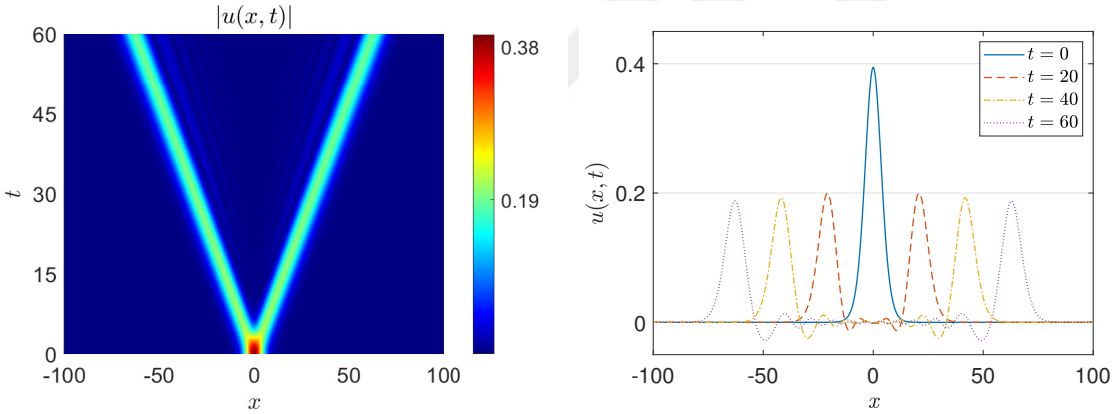


**Figure 5.3 :** The contour plot of single wave splitting for the quadratic nonlinearity (left panel), snapshots of the solitary wave at different times (right panel).

The computations are performed on the domain $\Omega = (-400, 400)$ up to $T = 60$ with $h = 0.5$ and $\tau = 0.005$. In the left panel of Figure 5.3, we show the dynamics of the solitary wave with amplitude $A = \frac{15}{38}$ and the null initial velocity for quadratic nonlinearity. Snapshots of the solutions at different times are illustrated in the right panel of Figure 5.3. We observe that the initial stationary wave splits up into two smaller diverging waves, one traveling towards the left and the other one to the right and the splitting leads to the creation of secondary solitary waves.

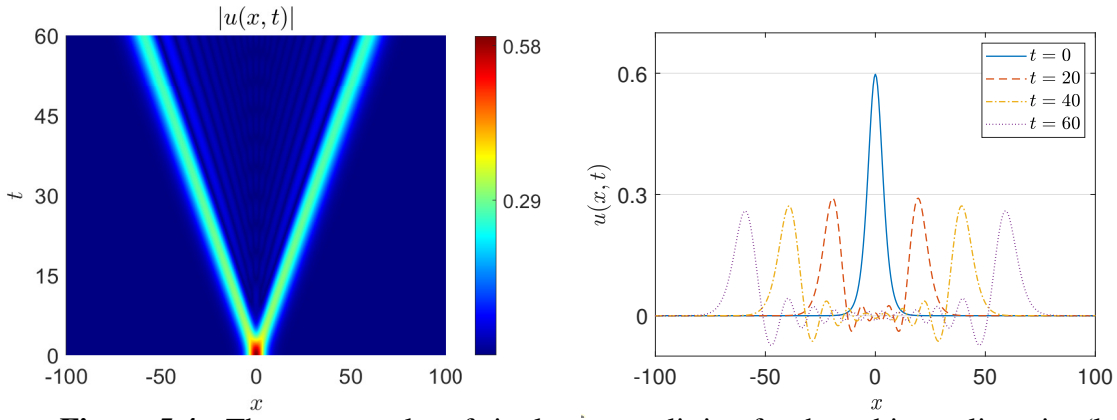


**Figure 5.4 :** The contour plot of single wave splitting for the cubic nonlinearity (left panel), snapshots of the solitary wave at different times (right panel).

The dynamic of the solitary wave with the amplitude $\sqrt{\frac{5}{14}}$ and the null initial velocity is depicted in Figure 5.4 for cubic nonlinearity. We observe that the dynamics are similar to quadratic nonlinearity. However, the secondary waves between the two main splitting waves become more discernible when the power of nonlinearity increases.

Since an analytical solution is not available for the single wave splitting experiments, we cannot give the errors for this experiment. However, the evolution of the change in the conserved quantity $\mathscr{M}$ is presented as a numerical validation of the proposed scheme in Figure 5.5. As expected, the conserved quantity remains constant in time.

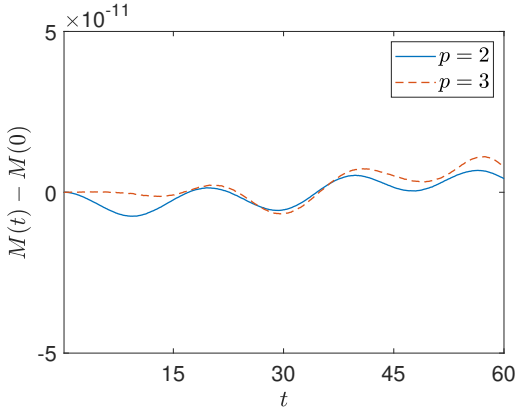


**Figure 5.5 :** The evolution of the change in the conserved quantity $\mathscr{M}$ for the single wave splitting.

### 5.3 Head-on Collision

In these numerical experiments, we use the initial data

$$\begin{aligned} u_0(x) &= \frac{15}{38}\operatorname{sech}^4\left(\frac{\sqrt{13}}{26}\Big[x+40\Big]\right)+\frac{15}{38}\operatorname{sech}^4\left(\frac{\sqrt{13}}{26}\Big[x-40\Big]\right) \\ u_1(x) &= \frac{15\sqrt{1729}}{2527}\operatorname{sech}^4\left(\frac{\sqrt{13}}{26}\Big[x+40\Big]\right)\tanh\left(\frac{\sqrt{13}}{26}\Big[x+40\Big]\right) \\ &\quad -\frac{15\sqrt{1729}}{2527}\operatorname{sech}^4\left(\frac{\sqrt{13}}{26}\Big[x-40\Big]\right)\tanh\left(\frac{\sqrt{13}}{26}\Big[x-40\Big]\right) \end{aligned}$$

for quadratic nonlinearity and

$$\begin{aligned} u_0(x) &= \sqrt{\frac{5}{14}}\operatorname{sech}^2\left(\frac{\sqrt{5}}{10}\Big[x+40\Big]\right)+\sqrt{\frac{5}{14}}\operatorname{sech}^2\left(\frac{\sqrt{5}}{10}\Big[x-40\Big]\right) \\ u_1(x) &= \frac{5\sqrt{6}}{42}\operatorname{sech}^2\left(\frac{\sqrt{5}}{10}\Big[x+40\Big]\right)\tanh\left(\frac{\sqrt{5}}{10}\Big[x+40\Big]\right) \\ &\quad -\frac{5\sqrt{6}}{42}\operatorname{sech}^2\left(\frac{\sqrt{5}}{10}\Big[x-40\Big]\right)\tanh\left(\frac{\sqrt{5}}{10}\Big[x-40\Big]\right) \end{aligned}$$

for cubic nonlinearity by taking $\eta_1 = \eta_2 = 1$.

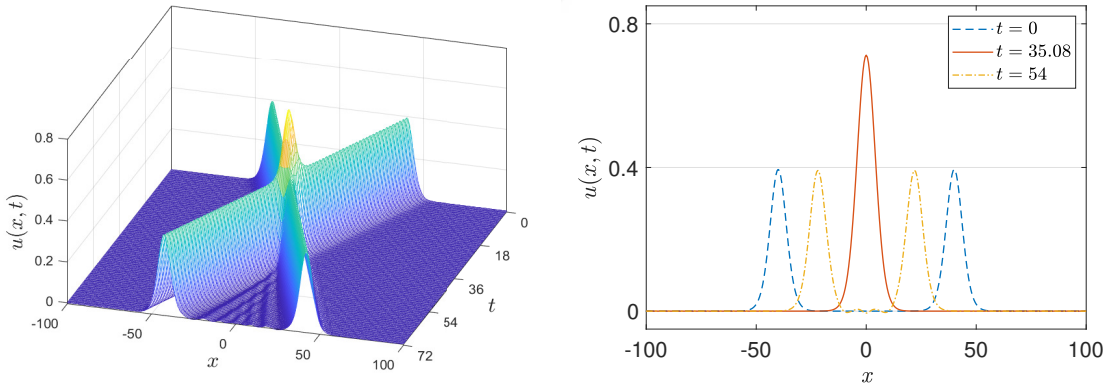


**Figure 5.6 :** The surface plot of the head-on collision of two solitary waves for the quadratic nonlinearity (left panel), snapshots of the solution at different times (right panel).

The computations are performed on the domain $\Omega = (-400, 400)$ up to $T = 72$ with $h = 0.5$ and $\tau = 0.005$. In the left panel of Figure 5.6, we show the head-on collision of two solitary waves with equal amplitudes for quadratic nonlinearity. We see the oscillating secondary waves. Therefore, the interaction is inelastic. The numerical solution at different times is shown in the right panel of Figure 5.6. The collision

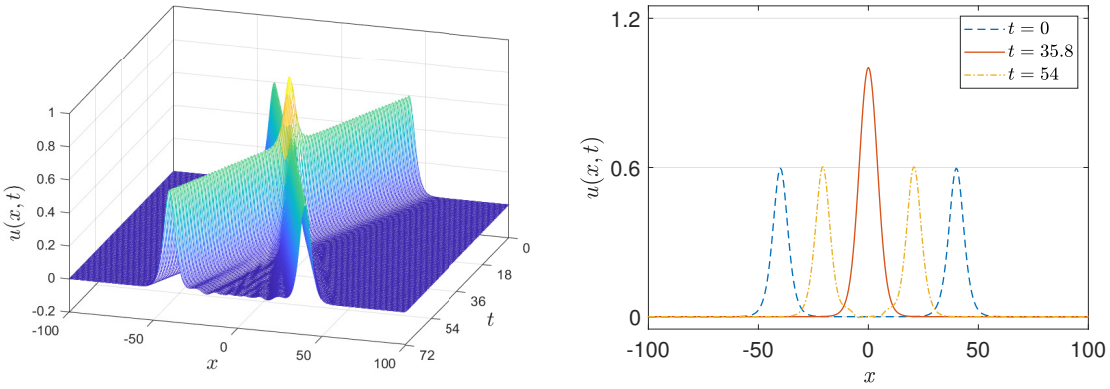


**Figure 5.7 :** The surface plot of the head-on collision of two solitary waves for the cubic nonlinearity (left panel), snapshots of the solution at different times (right panel).

occurs at around $t = 35.08$ with the largest amplitude which is smaller than the sum of the two initial amplitudes. We observe that the small secondary waves are emitted after collision time. We also compute that the amplitudes of secondary waves are smaller than 0.006.

The head-on collision of two solitary waves for cubic nonlinearity is illustrated in Figure 5.7, we see that the collision is inelastic and the interaction is similar to quadratic nonlinearity. We observe that the amplitudes of secondary waves are smaller than 0.0098. We also observe that the amplitudes of secondary waves which occur after the collision are less than 2% of the amplitude of the waves at the initial time for both quadratic and cubic nonlinearity. Figure 5.8 shows that the conserved quantities for the head-on collision of two solitary waves remain constant in time for both cases. These results provide a valuable check on the numerical results.

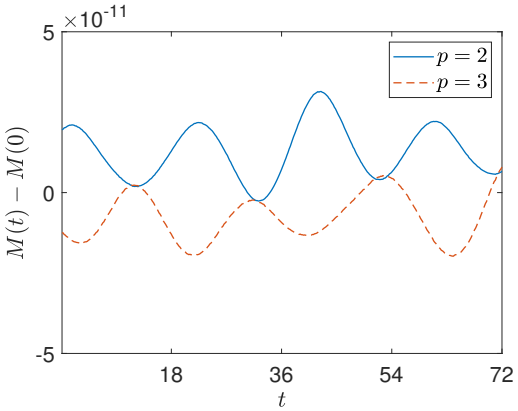


**Figure 5.8 :** The evolution of the change in the conserved quantity $\mathscr{M}$ for the head-on collision of two solitary waves.

# 6. CONCLUSION

## 6.1 Conclusion

As a summary, we derived a new exponential wave integrator sine pseudo-spectral (EWI-SP) method for the higher-order Boussinesq equation. It was shown that the method is fully-explicit and has fourth-order accuracy in time and spectral accuracy in space. We rigorously carried out error analysis and established error bounds in the Sobolev spaces. The performance of the EWI-SP method is illustrated by examining the long-time evolution of the single solitary wave, single wave splitting and head-on collision of solitary waves. Numerical experiments confirm the theoretical results.

## 6.2 Future Discussions

In this thesis, we showed how we obtain the numerical solutions of the higher-order Boussinesq equation but we didn't generalize the method for similar problems. The EWI-SP method may also be implemented for the other equations that are reducible to second-order ordinary differential equations by the sine pseudo-spectral approximation. Furthermore, we presented the numerical solutions for the higher-order Boussinesq equation which is (1+1) dimensional equation. The EWI-SP method may be arranged for higher dimensional equations. Lastly, we solve single equation in the thesis. The EWI-SP method may be generalized for the numerical solutions of the system of equations.

Briefly, future studies may focus on generalizing the EWI-SP method to the cases described above.

## REFERENCES


[1] **Rosenau, P.** (1988). Dynamics of dense discrete dystems: High order effects, *Progress of Theoretical Physics*, *79*(5), 1028–1042.

[2] **Duruk, N.**, **Erkip, A. and Erbay, H.A.** (2008). A higher-order Boussinesq equation in locally non-linear theory of one-dimensional non-local elasticity, *IMA Journal of Applied Mathematics*, *74*(1), 97–106.

[3] **Schneider, G.** (1998). The long wave limit for a Boussinesq equation, *SIAM Journal on Applied Mathematics*, *58*(4), 1237–1245.

[4] **Boussinesq, J.** (1872). Théorie des ondes et des remous qui se propagent le long d'un canal rectangulaire horizontal, en communiquant au liquide contenu dans ce canal des vitesses sensiblement pareilles de la surface au fond., *Journal de Mathématiques Pures et Appliquées*, *17*, 55–108.

[5] **Bogolubsky, I.** (1977). Some examples of inelastic soliton interaction, *Computer Physics Communications*, *13*(3), 149–155.

[6] **Makhankov, V.** (1978). Dynamics of classical solitons (in non-integrable systems), *Physics Reports*, *35*(1), 1–128.

[7] **Oruc, G. and Muslu, G.M.** (2019). Existence and uniqueness of solutions to initial boundary value problem for the higher order Boussinesq equation, *Nonlinear Analysis: Real World Applications*, *47*, 436–445.

[8] **Hasanoğlu, Y. and Özemir, C.** (2021). Group classification and exact solutions of a higher-order Boussinesq equation, *Nonlinear Dynamics*, *104*(3), 2599–2611.

[9] **Bratsos, A.G.** (2007). A second order numerical scheme for the solution of the one-dimensional Boussinesq equation, *Numerical Algorithms*, *46*(1), 45–58.

[10] **Ortega, T. and Sanz-Serna, J.M.** (1990). Nonlinear stability and convergence of finite-difference methods for the "good" Boussinesq equation, *Numerische Mathematik*, *58*(1), 215–229.

[11] **Cheng, K.**, **Feng, W.**, **Gottlieb, S. and Wang, C.** (2014). A Fourier pseudospectral method for the "good" Boussinesq equation with second-order temporal accuracy, *Numerical Methods for Partial Differential Equations*, *31*(1), 202–224.

[12] **de Frutos, J.**, **Ortega, T. and Sanz-Serna, J.M.** (1991). Pseudospectral method for the "good" Boussinesq equation, *Mathematics of Computation*, *57*(195), 109–122.

[13] **Zhang, C.**, **Wang, H.**, **Huang, J.**, **Wang, C. and Yue, X.** (2017). A second order operator splitting numerical scheme for the “good” Boussinesq equation, *Applied Numerical Mathematics*, *119*, 179–193.

[14] **Su, C. and Yao, W.** (2020). A Deuflhard-type exponential integrator Fourier pseudo-spectral method for the “good” Boussinesq equation, *Journal of Scientific Computing*, *83*(1).

[15] **Bratsos, A.** (2009). A predictor–corrector scheme for the improved Boussinesq equation, *Chaos, Solitons & Fractals*, *40*(5), 2083–2094.

[16] **Irk, D. and Dağ, I.** (2009). Numerical simulations of the improved Boussinesq equation, *Numerical Methods for Partial Differential Equations*, *26*(6), 1316–1327.

[17] **Lin, Q.**, **Wu, Y.H.**, **Loxton, R. and Lai, S.** (2009). Linear B-spline finite element method for the improved Boussinesq equation, *Journal of Computational and Applied Mathematics*, *224*(2), 658–667.

[18] **Borluk, H. and Muslu, G.M.** (2014). A Fourier pseudospectral method for a generalized improved Boussinesq equation, *Numerical Methods for Partial Differential Equations*, *31*(4), 995–1008.

[19] **Shokri, A. and Dehghan, M.** (2010). A not-a-knot meshless method using radial basis functions and predictor–corrector scheme to the numerical solution of improved Boussinesq equation, *Computer Physics Communications*, *181*(12), 1990–2000.

[20] **Mohebbi, A.** (2012). Solitary wave solutions of the nonlinear generalized Pochhammer–Chree and regularized long wave equations, *Nonlinear Dynamics*, *70*(4), 2463–2474.

[21] **Wang, Q.**, **Zhang, Z.**, **Zhang, X. and Zhu, Q.** (2014). Energy-preserving finite volume element method for the improved Boussinesq equation, *Journal of Computational Physics*, *270*, 58–69.

[22] **Yan, J.**, **Zhang, Z.**, **Zhao, T. and Liang, D.** (2018). High-order energy-preserving schemes for the improved Boussinesq equation, *Numerical Methods for Partial Differential Equations*, *34*(4), 1145–1165.

[23] **Su, C. and Muslu, G.M.** (2021). An exponential integrator sine pseudospectral method for the generalized improved Boussinesq equation, *BIT Numerical Mathematics*, *61*(4), 1397–1419.

[24] **Oruc, G.**, **Borluk, H. and Muslu, G.M.** (2017). Higher order dispersive effects in regularized Boussinesq equation, *Wave Motion*, *68*, 272–282.

[25] **Bao, W. and Dong, X.** (2011). Analysis and comparison of numerical methods for the Klein-Gordon equation in the nonrelativistic limit regime, *Numerische Mathematik*, *120*(2), 189–229.

[26] **Zhao, X.** (2015). On error estimates of an exponential wave integrator sine pseudospectral method for the Klein-Gordon-Zakharov system, *Numerical Methods for Partial Differential Equations*, *32*(1), 266–291.

[27] **Zhao, X.** (2016). An exponential wave integrator pseudospectral method for the symmetric regularized-long-wave equation, *Journal of Computational Mathematics*, *34*(1), 49–69.

[28] **Bao, W. and Cai, Y.** (2014). Uniform and optimal error estimates of an exponential wave integrator sine pseudospectral method for the nonlinear Schrödinger equation with wave operator, *SIAM Journal on Numerical Analysis*, *52*(3), 1103–1127.

[29] **Li, X. and Zhang, L.** (2018). Error estimates of a trigonometric integrator sine pseudo-spectral method for the extended Fisher-Kolmogorov equation, *Applied Numerical Mathematics*, *131*, 39–53.

[30] **Li, J.** (2021). Error analysis of a time fourth-order exponential wave integrator Fourier pseudo-spectral method for the nonlinear Dirac equation, *International Journal of Computer Mathematics*, *99*(4), 791–807.

[31] **Ji, B. and Zhang, L.** (2019). Error estimates of exponential wave integrator Fourier pseudospectral methods for the nonlinear Schrödinger equation, *Applied Mathematics and Computation*, *343*, 100–113.

[32] **Ji, B. and Zhang, L.** (2020). A fourth-order exponential wave integrator Fourier pseudo-spectral method for the Klein-Gordon equation, *Applied Mathematics Letters*, *109*, 106519.

[33] **Wang, Y. and Zhao, X.** (2016). *Symmetric high order Gautschi-type exponential wave integrators pseudospectral method for the nonlinear Klein-Gordon equation in the nonrelativistic limit regime*, `1611.01550`.

[34] **Canuto, C.**, **Hussaini, M.Y.**, **Quarteroni, A. and Zang, T.A.** (2007). *Spectral Methods: Fundamentals in Single Domains*, ISSN, Springer-Verlag, Berlin Heidelberg.

[35] **Adams, R. and Fournier, J.** (2003). *Sobolev Spaces*, ISSN, Elsevier Science, Amsterdam.

[36] **Chartier, P.**, **Méhats, F.**, **Thalhammer, M. and Zhang, Y.** (2016). Improved error estimates for splitting methods applied to highly-oscillatory nonlinear Schrödinger equations, *Mathematics of Computation*, *85*(302), 2863–2885.

[37] **Royden, H.L. and Fitzpatrick, P.** (1968). *Real Analysis*, ISSN, Macmillan, New York.

## CURRICULUM VITAE

**Name SURNAME:** Melih Cem ÇANAK

**EDUCATION:**

- **B.Sc.:** 2020, Istanbul Technical University, Faculty of Mechanical Engineering, Mechanical Engineering
- **B.Sc.:** 2020, Istanbul Technical University, Faculty of Science and Letters, Mathematical Engineering
- **M.Sc.:** 2024, Istanbul Technical University, Graduate School, Mathematical Engineering

**PROFESSIONAL EXPERIENCE AND REWARDS:**

- 2021-2022, Research Assistant, Işık University
- 2022-present, Research Assistant, İstanbul Technical University

**PUBLICATIONS, PRESENTATIONS AND PATENTS ON THE THESIS:**

- **Canak, M. C.**, Muslu G. M. (2023). An exponential wave integrator sine pseudo-spectral method for the higher-order Boussinesq equation with fourth-order temporal accuracy, *International Graduate Research Symposium IGRS'23*, May 2-5, 2023 Istanbul, Turkey.
- **Canak, M. C.**, Muslu G. M. (2023). Yüksek Mertebe Boussinesq Denkleminin Sayısal Çözümleri İçin Sinüs Sözde-Spektral Yönteminin Hata Analizi, *35. Ulusal Matematik Sempozyumu UMS 2023*, September 4-8, 2023 Edirne, Turkey.
- **Canak, M. C.**, Muslu G. M. (2024). Error analysis of the exponential wave integrator sine pseudo-spectral method for the higher-order Boussinesq equation, *Numerical Algorithms* (accepted).